

Efficient Acoustic Modelling of Large Spaces using Time Domain Methods

The Evaluation of Three Time Domain Numerical Methods for Solving the Acoustic
Wave Equation, Applied to Solving Large Domains

Simon Durbridge

May 2017

UNIVERSITY *of* DERBY



Faculty of Arts, Design and Technology
School of Engineering and Technology
The University of Derby

Submitted in part-fulfilment of the requirements for the MSc in Audio Engineering

Summary

Time domain numerical for solving acoustic equations have been of continuing interest and development since early work by key figures such as Botteldooren [1]. Some distinct disadvantages to these methods mean that they are often only implemented for low frequency modelling, and in hybrid schemes such as the one presented by Mourik and Murphy [2]. Ray based acoustic modelling methods may be no more efficient when modelling multiple sources and receivers in large domains, as the number of rays required for accurate simulation can become very large. In this study three time domain numerical methods are implemented, the finite difference time domain method, the sparse finite difference time domain method and the psudospectral time domain method. The execution times for these three methods are evaluated in domains of varying size, using commonly available computing resources. It is found that the pseudospectral time domain method is the fastest per time step of the three methods, when solving for very large domains i.e. millions cells in volume. This is potentially due to the nature of differentiation by multiplication in the frequency domain.

Acknowledgements

I would like to thank my supervisor Dr Adam Hill for his friendly, diligent and understanding guidance throughout my academic career. He has guided and steadied my hand through all circumstances even through my often difficult character, and it is on his work that this work has evolved. His honest and poignant observations have helped my confidence immensely, and for his help I am exceedingly grateful.

I would like to thank my family and my partner Bethany, for all of their help, support and understanding throughout the course of this masters degree. Without Beths constant and accommodating support, I would be nothing more than a ruined mess and this work wouldn't have even been started.

I would like to thank all those whose work I have built from, and those who have provided guidance. Particularly Jamie Angus, Damian Murphy and Raymond Rumpf for their correspondence. I would also like to thank the team at Bowers and Wilkins for their help and support.

Finally I would once again like to thank and congratulate William and Yasmin Draffin. Without these two people I would not have entered the world of academia, and I wouldn't be where I am today.

Contents

1	Introduction	6
1.1	Problem Definition	6
1.2	Aim of the Study	7
1.3	Format of the Report	7
2	Acoustic Principals	8
2.1	The Acoustic Wave Equation	8
2.1.1	Wave Equation In One Dimension	9
2.2	Acoustic Properties of Interest in This Study	12
2.2.1	Inverse Square Law & Propagation time	12
2.2.2	Reverberation	13
2.2.3	Room Modes	15
3	Time Domain Numerical Methods	18
3.1	Finite Difference Time Domain Method	18
3.1.1	Introduction to the Finite Difference Time Domain Method	19
3.1.2	The Finite Difference Time Domain Method Applied To The Acoustic Wave Equation	19
3.1.3	Field Calculation	20
3.1.4	Boundary Handling	21
3.1.5	Block Diagram	23
3.1.6	Example Update Function	24
3.1.7	Stability	25
3.2	Sparse FDTD	26
3.2.1	Introduction to the Sparse Finite Difference Time Domain Method	26
3.2.2	Acoustic Implementation of SFDTD in Two Dimensions	27
3.3	Pseudo-Spectral Time Domain Method	33
3.3.1	A Background to the Pseudo-Spectral Time Domain Method	33
3.3.2	Block Diagram	33
3.3.3	The Pseudospectral Time Domain Method Applied To The Wave Equation	35
3.3.4	Absorbing Boundary Conditions	37
3.3.5	Partially Absorbing Boundary Conditions	39
3.4	Sound Source Terms	40

4 Validation	42
4.1 Validation Strategy	42
4.1.1 The Domain	42
4.2 Results	44
4.2.1 FDTD Simulation Results	44
4.2.2 SFDTD Simulation Results	44
4.2.3 PSTD Simulation Results	46
4.3 Validating The SFDTD Method	47
5 Execution Time and Analysis	49
5.1 Results	49
5.2 Analysis	52
5.3 Code Profiling	53
6 Conclusion and Further Work	57
6.1 Conclusion	57
6.2 Further Work	58
A Code Listing	64

List of Figures

1.1	2D Representation of Ray Tracing Concept [3]	6
2.1	Room Modes up to Schroeder Frequency for a Small Rectangular Room	16
2.2	Schroeder frequency as a function of domain size and RT60	17
3.1	Example Mesh Plot of an FDTD Simulation With Two Sources	18
3.2	Visualization of a 2D FDTD Scheme With Offset Grids [4]	20
3.3	Example Plot of an FDTD Simulation With Reflection From an Obstable	22
3.4	Window Function	28
3.5	Pressure Function	28
3.6	Caption place holder	28
3.7	Examples of an Expanding Wave in an SFDTD Simulation	28
3.8	Window of an expanding wave in an SFDTD simulation	29
3.9	Window of an expanding wave in an SFDTD simulation	30
3.10	Smoothed rate of time step execution for the SFDTD method during simulations, for different threshold levels	31
3.11	Single source SFDTD simulation in a small room with nodes and anti-nodes present	32
3.12	2D Differentiation Matrix in 1 Direction for a PSTD Simulation	36
3.13	PSTD 2D PML Coefficient Matrix	39
3.14	Example Plot of a 2D PSTD Simulation With Reflections	40
4.1	Room Modes up to Schroeder Frequency for a Small Rectangular Room	43
4.2	Validation data of FDTD simulation	44
4.3	Validation data of PSTD simulation With MLS Source	46
4.4	Validation data of PSTD simulation With Tone Burst Source	46
4.5	Validation data of PSTD simulation	48
5.1	Execution times for FDTD simulations in domains of increasing size .	50
5.2	Execution times for PSTD simulations in domains of increasing size .	51
5.3	Execution times for SFDTD simulations in domains of increasing size	52
5.4	Code execution time profile of PSTD functions	53
5.5	Code execution time profile of FDTD functions	54
5.6	Code execution time profile of SFDTD functions	55

Chapter 1

Introduction

Modelling and replicating the effects of acoustic systems has been of continued interest to a number of industries, from the creation of scale models for concert halls to the generation of individualised audio in video games [5]. Acoustic modelling is not only a tool for those wishing to design acoustic systems, but may be of increasing interest for those wishing to experience an acoustic system¹ from the comfort of the home or office [6]. Simulating the acoustic behaviour of large systems with multiple sources and receivers may not be a trivial undertaking, with significant computational resources required to model such systems.

1.1 Problem Definition

Current commercially available acoustic modelling tools for large (cathedrals, arenas, video game maps etc) electroacoustic simulations rely on assumptions based around plane wave propagation. These models are only accurate when assuming that detail of the domain features are significantly larger than the wavelengths of interested, and that no diffraction effects occur [7]. These ray based methods such as the image source method and ray or beam tracing methods approximate the performance of the system and simulation domain without solving the full wave physics of an acoustic system [8]. These methods have been successfully used to approximate large systems at mid and high frequencies, but may not accurately simulate low frequency wave propagation and wave interaction.

Wave based acoustic modelling methods such as the Finite Element Method (FEM) and Boundary Element Method (BEM) have been are currently implemented in com-

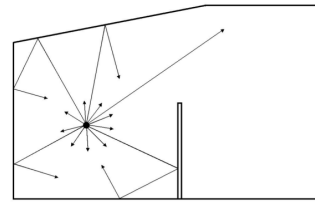


Figure 1.1: 2D Representation of Ray Tracing Concept [3]

¹In this context we consider an acoustic system as whole i.e. sound sources, receivers, the propagation medium and the domain boundaries

mercial software packages, and are often used to model complex acoustic systems such as loudspeakers and other transducers. However, these packages are difficult to apply to simulating large domain problems, due to the computational resource limitations that are inherent with numerical solutions to wave based methods. Modelling large 3D domains even at lower frequencies can have extreme memory requirements, and may also require significant computation time to 'crunch the numbers' and solve for adequate amounts of time. One commercial FEM package known as Comsol has recently added ray tracing to the acoustics tools, potentially to accommodate this restriction [9].

1.2 Aim of the Study

The aim of this study is to test three numerical methods of solving the acoustic wave equation that result in time domain solutions. These methods will be implemented in the Matlab ® language tested for speed of time step execution with consecutively large domains. The methods of interested in this studying are the finite difference time domain method (FDTD), the sparse finite difference time domain method (SFDTD) and the pseudospectral time domain method (PSTD). The outcome of this study will be the identification of a method that may warrant further optimisation for large domains and could be potentially used for accurately modelling large electroacoustic systems and venues. To summaries, these are the objectives in this project:

- Explore and implement FDTD method in 1D, 2D and 3D
- Explore and implement PSTD method in 1D, 2D and 3D
- Implement PSTD method partially absorbing boundaries
- Explore and implement SFDTD method in 1D, 2D and if possible 3D
- Validate these models propagate sound appropriately
- Benchmark the execution speed for these methods in different size models
- Write a report detailing the study

1.3 Format of the Report

At first the acoustic wave equation will be derived, and some properties of large room acoustics will be discussed. Following this the finite difference time domain, sparse finite difference time domain and pseudo spectral time domain methods for solving the acoustic wave equation will be introduced, including equation derivation and Matlab code examples. Following this the software validation will be discussed, and finally the time step execution times will be evaluated including profiling to determine the slowest part of code execution.

Chapter 2

Acoustic Principles

Acoustics is a branch of physics¹ that aims to characterise behaviours of Newton's second law of motion applied to mechanical wave propagation and obeying the physical conservation law [10]. This characterisation of sound propagation is intrinsically linked to many other disciplines of science and engineering, as well as psychological and perceptual study. In this section we will review the acoustic wave equation, and discuss some acoustic equations of interest in large room electroacoustics.

2.1 The Acoustic Wave Equation

Acoustic waves are classified as fluctuations of pressure in a given medium, manifesting as longitudinal waves of high and low pressure and air density [11]. These fluctuations are often cyclical in nature around an ambient pressure that is sometimes assumed to be 1 atmospheric pressure at sea level or $101.35kPa$. Similar to the behaviour of heat convection or fluid diffusion, these cyclical fluctuations propagate and spread through the medium of interest, decaying towards a resting steady state. It is possible to calculate an approximate solution to the propagation of pressure through a space, by solving a system of second order partial differential equations that can be collected into a 'Wave Equation'. Below, we will introduce the three building blocks of the wave equation in one dimensional space. These building blocks are Newton's Second Law of Motion, the gas law, and the laws of conservation of mass.

In the McGraw-Hill Electronic and Electrical Engineering Series of books, the late Leo Beranek authored the Acoustics volume [10]. This reference text contains an elegant summary of the wave equation in 1 dimension in standard notation, and 3 dimensions in vector notation. Rienstra published an introduction to acoustics text [12] that takes a strong stance from a fluid dynamics perspective, and is well worth reviewing for a more in-depth derivation than is presented in this text. To consider the wave equation, we should use the analogy of a small volume of gas, within a significantly larger

¹though often considered to be interdisciplinary

homogeneous medium. The faces of the volume are frictionless, and only the pressure at any face impacts on the gas inside the volume.

2.1.1 Wave Equation In One Dimension

Equation Of Motion

Sound pressure p propagates across the larger medium like a plane wave, from one side to the other in the x direction at a rate equal to the change in space: $\frac{\delta p}{\delta x}$
Force acting on the volume in the positive x direction can thus be described as:

$$-(\frac{\delta p}{\delta x} \Delta x) \Delta y \Delta z \quad (2.1)$$

Assuming that the balance of force across the volume over a slice of time is equal to the unit size of the volume and the speed of the wave.

A positive gradient causes acceleration in the $-x$ direction, and a negative gradient causes acceleration of the volume in the $+x$ direction.

Force f per unit volume V is given by dividing both sides of the previous equation by the area of the volume:

$$V = \Delta x \Delta y \Delta z \frac{f}{V} = -\frac{\delta p}{\delta x} \quad (2.2)$$

Newton's second law of motion dictates that the rate of change of momentum in the volume must balance with force per unit volume, and we assume the mass M of gas in the volume is constant. The force mass balance can be described as:

$$\frac{f}{V} = -\frac{\delta p}{\delta x} = \frac{M}{V} \frac{\delta u}{\delta t} = \rho' \frac{\delta u}{\delta t} \quad (2.3)$$

Where u is the velocity of gas in the volume, ρ' is the density of the gas, and $M = \rho' V$ is the mass of gas in the volume.

If the change in density of gas in the volume is sufficiently small, the ρ' will be approximately equal to the average density ρ_0 , thus simplifying the equations above to:

$$-\frac{\delta p}{\delta x} = \rho_0 \frac{\delta u}{\delta t} \quad (2.4)$$

Which is the momentum equation.

Gas Law

This approximation may be appropriate as long as the absolute maximum pressure is relatively low, so that the behaviour of the air may be assumed to be linear and other assumption can be made that will be discussed shortly.

Assuming that the gas in the volume is ideal, the gas law $PV = RT$ should hold true. Here, T is the temperature in degrees Kelvin, and R is a constant based on the mass of

the gas. For this approximation we assume that the system is adiabatic and that compression and expansion are sufficiently fast to make the thermal effects negligible, and that T and R are lumped into a gas constant which for air is $\gamma \approx 1.4$.

In differential form the relationship between pressure and volume for an adiabatic expansion of the volume is $\frac{\delta P}{P} = -\frac{\gamma \delta V}{V}$ i.e. changes in pressure scale with changes in volume by this γ value.

If perturbations in pressure and volume due to a sound wave (p for pressure and τ for volume respectively) are sufficiently small compared to the rest values P_0 and V_0 , the time based derivative of the above equation can be written as follows:

$$\frac{1}{P_0} \frac{\delta p}{\delta t} = -\frac{\gamma}{V_0} \frac{\delta \tau}{\delta t} \quad (2.5)$$

This equation shows the balance between the proportional changes in pressure and volume over time, with a scaling of the change of the volume by the constant γ .

Conservation Of Mass

As this wave equation is concerned with the transport of pressure within a volume and not just the aggregate pressure of the volume with respect to the surrounding medium, a continuity expression must be applied. The conservation of mass states that the total mass of gas in the volume must remain constant. This conservation law brings a unique relationship between discrete velocities at the boundary of the volume. If the volume is displaced by some rate ε_x , air particles at either boundary of the volume at some point in time must be displaced at an equal rate for the mass of the volume to remain constant. As such if the left side of the volume is displaced with a velocity, in a given time the particles at the right hand boundary must also be displaced. This general displacement term can be written as:

$$\varepsilon_x + \frac{\delta \varepsilon_x}{\delta x} \Delta x \quad (2.6)$$

The change of velocity with respect to the volumes dimension gives:

$$\tau = V_0 \frac{\delta \varepsilon_x}{\delta x} \Delta x. \quad (2.7)$$

Differentiating this with respect to time gives:

$$\frac{\delta \tau}{\delta t} = V_0 \frac{\delta u}{\delta x} \quad (2.8)$$

Where u is the instantaneous particle velocity.

Wave Equation

The one dimensional wave equation can be created by combining the above statements about Newtons second law of motion, the gas law and the continuity equation. The combination of the gas law and continuity equation gives:

$$\frac{\delta p}{\delta t} = -\gamma P_0 \frac{\delta u}{\delta x}. \quad (2.9)$$

Which differentiated with respect to time gives:

$$\frac{\delta^2 p}{\delta t^2} = -\gamma P_0 \frac{\delta^2 u}{\delta t \delta x}. \quad (2.10)$$

Differentiating the momentum equation derived above with respect to time gives:

$$-\frac{\delta^2 p}{\delta t^2} = \rho_0 \frac{\delta^2 u}{\delta x \delta t} \quad (2.11)$$

Combining the above equations gives the equation for pressure transport with respect to time:

$$\frac{\delta^2 p}{\delta x^2} = \frac{\rho_0}{\gamma P_0} \frac{\delta^2 p}{\delta t^2} \quad (2.12)$$

If c is defined as the speed of propagation in the medium of interest:

$$c^2 \approx \frac{\gamma P_0}{\rho_0} \quad (2.13)$$

This is true [10] when making the assumption that:

$$c \approx (1.4 \frac{10^5}{1.2})^{\frac{1}{2}} \quad (2.14)$$

Where:

- ambient air pressure at sea level is $10^5 Pa$
- 1.4 is the adiabatic constant γ (ratio of specific heats) for air
- the density of air $\rho_0 \approx 1.2 kg/m^3$

The 1 dimensional wave equation is defined in terms of pressure fluctuation over space for time as:

$$\frac{\delta^2 p}{\delta x^2} = \frac{1}{c^2} \frac{\delta^2 p}{\delta t^2} \quad (2.15)$$

This equation can also be expressed in terms of the instantaneous velocity in the volume over time as:

$$\frac{\delta^2 u}{\delta x^2} = \frac{1}{c^2} \frac{\delta^2 u}{\delta t^2} \quad (2.16)$$

In the above section the wave equation has been derived with forms of velocity and pressure as the independent variables. We have also shown that pressure, velocity,

displacement and density are related within the system of equations, by differentiating and integrating with respect to space and time. As these forms of the wave equation are intrinsically coupled, it is possible to leverage this coupling when generating a numerical solution to the wave equation. It is also important to note that a significant number of assumptions have been made when deriving these equations, and any solution to these equations may only be accurate when simulating a loss free, frictionless, homogeneous, ideal gas medium, where all perturbations are sufficiently small and fast that it is possible to reduce the complexity of the system.

2.2 Acoustic Properties of Interest in This Study

Having derived a wave equation to simulation acoustic propagation, it is important to have an understanding of what acoustic phenomena can be observed through solving the wave equation. This study is interested in solving large domains efficiently, and next section will discuss three components of acoustics behaviour that may relate to large room acoustics.

2.2.1 Inverse Square Law & Propagation time

As previously noted, sound propagates as longitudinal waves through a medium such as air or water. These waves are often conceptualised as simple rays [10] travelling through a space², much like planar waves. However, the properties of a sound source such as the directivity and shape can have a significant effect on the behaviour of sound wave propagation. An example of this is the difference in energy spread over distance for theoretically ideal point and line sources. Ideal point sources that propagate sound omni-directionally obey the inverse square law and propagate sound spherically, and ideal line sources do not as they propagate sound cylindrically. The inverse square law is sound propagations is defined as [13]

$$I = \frac{P}{4\pi r^2} \quad (2.17)$$

Where I is the intensity over the area of the sphere, P is the propagated energy at the source and r is the radius of the sphere i.e. the distance between the source and the point of inquiry. This equation denotes that as an acoustic pressure wave radiates outward like an expanding sphere, as the area of the surface of the sphere increase the energy-per-unit-area of the surface of the sphere decreases. That is, as r increases, I decreases, assuming P is a constant pressure of interest.

As ideal line sources propagate pressure waves cylindrically, the equation above can be modified to account for this change:

$$I = \frac{P}{2\pi r} \quad (2.18)$$

²It may be appropriate to often consider space to be 3 dimensional (3D), or a lower order approximation of a 3D space

These two similar equations show a change in relationship between acoustic power over distance for different acoustic sources. If you were to evaluate the change of I for different values of r with the point source equation, you would find that as r is doubled I decreases by $6dB$. Doing the same for the line source equation would yield a $3dB$ change. This is in part due to the fact that we assume the cylinder is infinitely long, and thus we are evaluating a 2D simplification of a 3D problem. The area of the cylinder for any value of r is less than the equivalent sphere, and so the theoretical distribution of energy is also reduced. This may be an important concept when considering the 2D approximation of 3D simulations in acoustic studies. Below is a graph showing the difference between intensity over distance for an ideal point and line source:

Although the wave equation considered and solved in this study is lossless i.e. we do not consider viscous or thermal losses in the basic linearised acoustic wave equation, we would expect to see a reduction in absolute pressure between a source and receiver. As sound travels at some finite distance over time c , we would also expect to see a uniform time between a wave being radiated from a source, and being recorded at some receiver location for all simulation methods³.

2.2.2 Reverberation

For this study we will consider spaces or domains of finite size. These domains have boundaries, and those boundaries will absorb and reflect sound waves by some proportion. In acoustic engineering the proportion of sound energy absorbed or reflected by a material is often described as an absorption or reflection coefficient α , which is often expressed as a normalised value between 0 (totally reflecting) and 1 (totally absorbing) [10]. When considering boundaries to have frequency dependent absorption characteristics, a series of absorption coefficients are often attributed to frequency bands and these coefficients are usually real and not complex numbers.

If a sound source propagates a signal of appropriate amplitude, the sound wave will reach the boundaries and be partially absorbed or reflected in reciprocal directions. These reflections will continue to reflect and scatter, and will eventually decay beyond audibility. The reverberant sound field is the steady-state of diffusely scattered sound energy (reflections), due to perturbation by a sound source in bounded space. The amplitude of the sound source and diffusely scattered reflections balance with the rate of decay (diffusion and absorption) of the sound field [14]. In this case, the sound field can be conceptually split proportionally into direct and reverberant fields.

Acoustic Absorption

The decay rate of a reverberant sound field is often quantified by the time taken for a steady state sound field to reduce in level by $60dB$, once the sound source has finished

³For an interesting review of the relationship between 1D, 2D and 3D sound propagation being derivative, please see the appendices

propagating. This is defined as the RT_{60} of the domain, and was first proposed by WC Sabine in 1900 [14]. There have been a multitude of expansions on Sabines original formula, notably the Norris-Eyring [15] equation which expanded the denominator of the reverberation time equation to allow for more realistically distributed absorption values above 0.1. The Norris-Eyring reverberation time equation is as follows [13]:

$$T = 0.161 \frac{V}{S\ln(1-\alpha)} \quad (2.19)$$

Where S is the surface area, V is the volume of the domain and α is the average absorption coefficient and can be calculated as such:

$$\alpha = ((S_{leftwall}\alpha_{leftwall}) + (S_{rightwall}\alpha_{rightwall}) + \dots) / S_{total}$$

The use of RT_{60} as the preferred metric of decay time is valid, assuming that the acoustics system is linear and time-invariant. A more comprehensive description of reverberation and overview of the associated parameters is given by Rossing [?].

Low order reflections often described as early reflections in relation to psychoacoustics, may occur above the steady state amplitude (echos) [14] if the steady state amplitude decreases appropriately. Early and strong reflections are of significant interest in acoustic modelling, and the auralization and perception of sound fields due to the cues humans receive from perception of them e.g. room size and source direction information.

Modified Hopkins-Stryker Equation

The Modified Hopkins-Stryker equation presented by Beranek and modified by Peutz and Davis [13] can be used to approximate the level of sound at a point in a domain due to the direct and reverberant sound field:

$$L_T = L_W + 10 \log \left(\frac{QM_e}{4\pi D_x^2} + \frac{4N}{S_\alpha M_a} \right) + K \quad (2.20)$$

Where:

- L_T = Total Level in dB
- L_W = Source Level at D_x in dB
- D_x = Distance To Receiver
- M_e = Direct Sound Modified i.e. Receiver Directivity
- Q = Directivity Factor of Source at D_x
- N = Radiated Acoustic Power
- M_a = Architectural Modifier to accommodate non-ideal absorption distribution
- S_α = Total Absorption in Sabines

- K = Unit scalar i.e. 10.5 for SI unit measurements such as meters

In large domains as D_x gets sufficiently far, L_W and N have to increase to meet the same levels as in a smaller space. Multiple loudspeakers with a high Q are often implemented to cover larger domains and further distances, thus increasing the value of N and dominating the reverberant term in the equation. As long as the M_a term is sufficiently small and the $S_\alpha M_a$ term is sufficiently high, the direct sound will dominate. However, in many large spaces such as arenas and stadiums, the S term will be very large and the α will often be significantly small, thus causing reverberation to be a problem in sound re-enforcement where the loudspeaker system is not powerful enough. The Modified Hopkins-Stryker equation relies on the same assumptions and ideal behaviour such as reverberation begin a stochastic process and the domain being ergodic i.e. absorption being evenly distributed, and so may not be an ideally accurate way to predict the behaviour.

2.2.3 Room Modes

As the domains of interest in this study are fully bounded (much like a room), sound waves propagating in the domain are subject to periodicity relative to the dimensions of the domain. That is at wavelengths relative to the dimensions of the domain, standing waves may occur within the domain i.e. there will be regions maximal and minimal pressure change at points $\frac{\lambda}{4}$ relative to a dimension of the domain, where λ is the spatial dimension of one cycle otherwise known as a wavelength. These standing waves are often called room modes, and for oblique modes in a 3 dimensional rectangular domain the frequencies of the modes can be calculated as such:

$$f_{n_x n_y n_z} = \frac{c}{2} \sqrt{\left(\frac{n_x}{l_x}\right)^2 + \left(\frac{n_y}{l_y}\right)^2 + \left(\frac{n_z}{l_z}\right)^2} \quad (2.21)$$

Where n_x, n_y, n_z is the order of the standing wave in the dimension.

These modes are defined in spatial reciprocity as axial, tangential and oblique, depending on the order of dimensions involved in the periodicity i.e. When using such an equation as that above to calculate the theoretical modes of a rectangular domain, a state table such as the one below may be used to define the $n_{x/y/z}$ order⁴ component of each term:

⁴number of cycles within the dimension

Mode Type	x order	y order	z order
Axial	0	0	1
Axial	0	1	0
Axial	1	0	0
Tangential	0	1	1
Tangential	1	1	0
Tangential	1	0	1
Oblique	1	1	1
Oblique	1	1	2
Oblique	1	2	1

In a room of the dimensions 5m by 4m by 3m, modes up to the 10th order may occur at the following frequencies:

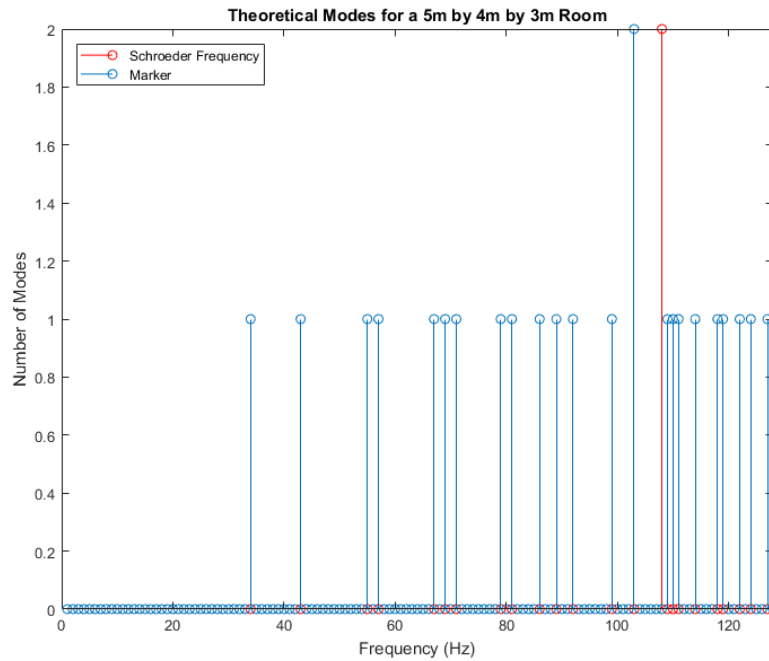


Figure 2.1: Room Modes up to Schroeder Frequency for a Small Rectangular Room

As modes occur at higher orders, the spatial change of the intensity of a particular frequency due to modes decreases to the point where the human ear may be insensitive to these changes. Further, at higher orders of modes the frequency density of modes may tend to converge, such that many modes occur around the same frequencies and so may appear to be diffusely occurring. The frequency at which modes tend to become difficult to observe by ear due to these properties for a particular domain is known as the

Schroeder frequency, and that is calculated by:

$$f_{Schroeder} = 2000 \sqrt{\frac{RT_{60}}{V}} \quad (2.22)$$

When considering the use of wave equation solver to compute acoustic propagation in large domains, it may be appropriate to consider calculating only up to a frequency of interest such as the Schroeder frequency using the wave method. This will reduce the required spatial resolution for the solution and thus will reduce total memory used and the time to completion per-time-step. However, calculating low frequency propagation may require to solve for longer total time to remain accurate [16]. In environments such as stadia, arenas and cathedrals, RT_{60} may vary from 1.2 to beyond 10s. The mesh plot below shows Schroeder frequency as a function of RT_{60} and room volume:

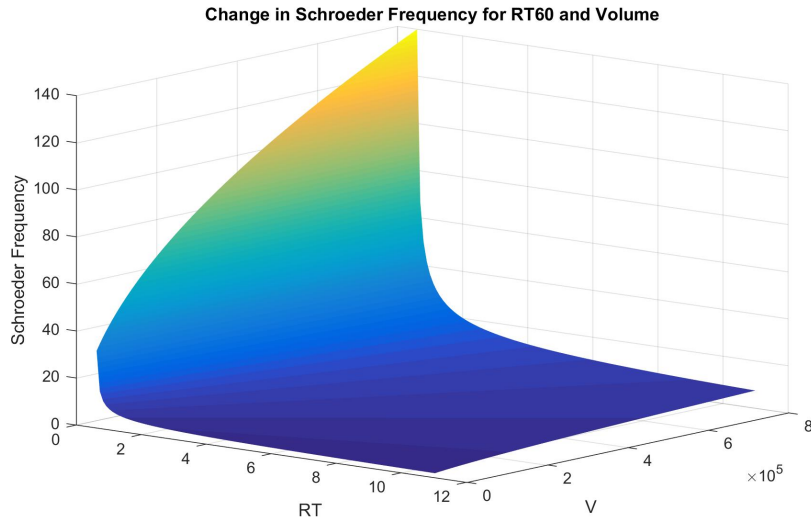


Figure 2.2: Schroeder frequency as a function of domain size and RT_{60}

Thus for very large domains with a short RT_{60} , modal analysis may be neither appropriate or necessary.

Chapter 3

Time Domain Numerical Methods

3.1 Finite Difference Time Domain Method

The Finite Difference Time Domain (FDTD) Method is a numerical method for solving partial differential equations. The power of this method lies in simplicity and flexibility, and it can be used to solve partial differential equations of varying complexity [17]. This chapter will discuss the application of the finite difference time domain method to the acoustic wave equation, including partially absorbing boundary conditions and the introduction of the sparse finite difference time domain method for acoustics.

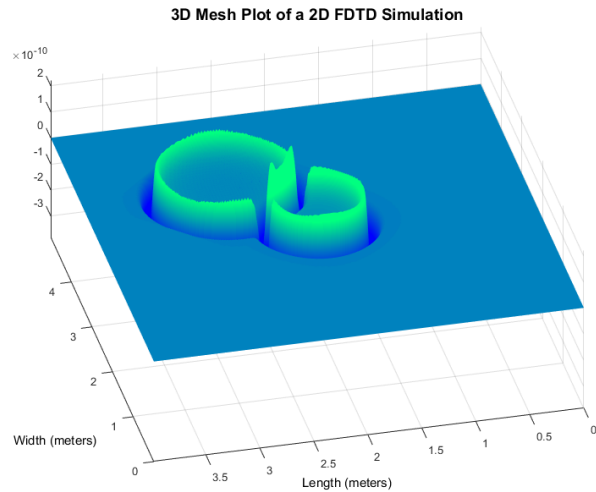


Figure 3.1: Example Mesh Plot of an FDTD Simulation With Two Sources

3.1.1 Introduction to the Finite Difference Time Domain Method

Methods for solving partial differential equations have been of significant and continued research since the early 1900s. Mathematicians such as Courant, Fiedrichs and Hrennikof undertook seminal work in the early 1920s that formed a base for much of the finite methods used today. The FDTD Method is a numerical method for solving time domain problems (often wave equations) with localised handling of spatial derivatives, and was first introduced for solving Maxwell's equations to simulate electromagnetic wave propagation by Yee [18].

Yee proposed a method for solving Maxwell's equations in partial differential form by applying them to staggered matrices in partial steps of time and space. These matrices represented the magnetic (H) and electric (E) fields, where the relationship between H and E means one perturbs the other. In this explicit formulation H and E are solved contiguously in a 'leapfrog' style, executing two sets of computations to solve for one time step. Multiple time steps would be solved from current time $t = 0$, in steps of dt to the end of simulation time T .

Each field is solved at half steps in time from the other, thus H for the current time step $t + \delta t$ is calculated using the H values one time step ago t , and the E values half a time step ago $t + \frac{\delta t}{2}$. These two fields are also solved using central finite differences in space, in a staggered grid format i.e. E at index x at time $t + \delta t$ is calculated using E at index x at time t , and the finite difference between the local discrete values of H at $x - \frac{\delta x}{2}$ and at $x + \frac{\delta x}{2}$ at time $t + \frac{\delta t}{2}$.

As such it is possible to apply a simple 'kernel' across many discrete points in a domain to simulate electromagnetic wave propagation.

In acoustics FDTD can be used to simulate a wide range of problems such as diffraction and diffusion, aeroacoustic, meteorological & environmental and mixed medium, without having to perform multiple simulations for different frequencies or simulation characteristics¹.

3.1.2 The Finite Difference Time Domain Method Applied To The Acoustic Wave Equation

The FDTD method applied to solving the acoustic wave equation follows a similar form to that of solving Maxwells Equations with FDTD [17]. Botteldoorens [19] seminal work applied the FDTD method to the acoustic wave equations for both Cartesian and quasi-Cartesian grid systems. As previously described in the room acoustics section, the linear acoustic wave equation is based on Newton's second law of motion, the gas law and the conservation of mass. The equation has the following form for changes in the pressure and velocity respectively within a volume:

¹as would have to be required in frequency domain simulations such as some Finite Element and Boundary Element simulations

$$\frac{\delta^2 p}{\delta t^2} = \frac{1}{c^2} \frac{\delta^2 p}{\delta t^2} \quad (3.1)$$

$$\frac{\delta^2 u}{\delta t^2} = \frac{1}{c^2} \frac{\delta^2 u}{\delta t^2} \quad (3.2)$$

As pressure p and velocity u have a reciprocal relationship in a similar way to H and E , it is possible to rearrange the acoustic wave equation to reflect this relationship for an FDTD computation.

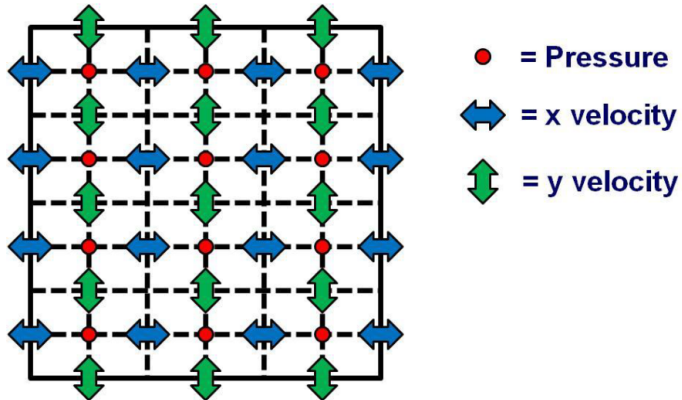


Figure 3.2: Visualization of a 2D FDTD Scheme With Offset Grids [4]

3.1.3 Field Calculation

When treating the 1 dimensional linear acoustic wave equation with the FDTD method, it is possible to treat the p and u terms separately in time using the opposing terms for reciprocal calculation. As such, the p and u terms are reformulated as follows:

$$\frac{\delta^2 p}{\delta t^2} = p - \frac{\delta t}{\rho_0 \delta x} \frac{\delta^2 u}{\delta t^2} \quad (3.3)$$

$$\frac{\delta^2 u}{\delta t^2} = u - \frac{\delta t}{\rho_0 \delta x} \frac{\delta^2 p}{\delta t^2} \quad (3.4)$$

This formulation is not in discrete time and space as is necessary when applying the FDTD method. As the FDTD method relies on solving local finite difference approximations across a domain of interest, it is important to define a space and time index referencing method. In many mathematical texts, time step indexing is often represented by an i notation, and spatial indexing often uses the j, k, l notation. For the sake of simplicity, in this study t will denote the time step index, and x, y and z will denote spatial indexing in each dimension in a similar way to the standard world coordinates system of many computer aided design packages.

Following an implementation of the acoustic FDTD method by Hill [4], the following

discrete time and space p and u equations can be described:

$$u_x^{t+\frac{\delta t}{2}} = u_x^{t-\frac{\delta t}{2}} - \frac{\delta t}{\rho \delta x} \left[p_{x+\frac{\delta x}{2}}^t - p_{x-\frac{\delta x}{2}}^t \right] \quad (3.5)$$

$$p_x^{t+\frac{\delta t}{2}} = p_x^{t-\frac{\delta t}{2}} - \frac{c^2 \rho \delta t}{\delta x} \left[u_{x+\frac{\delta x}{2}}^t - u_{x-\frac{\delta x}{2}}^t \right] \quad (3.6)$$

These update equations are developed for used with two matrices, one for pressure values and one for velocity values. The size of these matrices is determined by the size of the domain of interest and the spatial step size. The spatial step size is determined by the highest frequency of interest and the number of grid points required per wavelength, which is often regarded as being between 6 and 10 points in much FDTD literature. The spatial step size has a significant impact on both simulation stability and execution time, and is discussed further in the report.

3.1.4 Boundary Handling

As a significant part of room acoustic simulation involves analysing the effects of reverberation, so it may be important to model a boundary (wall, ceiling, floor) that will absorb and reflect some proportion of energy that is at the boundary. This can be handled by calculating partial derivatives at the boundaries of the domain based on the acoustic impedance of the boundaries [20] [4] i.e. boundaries are handled at velocity points where one pressure point is available for the differentiation. p , u and impedance z are often applied in a relationship similar to Ohms law $v = i * r$. The absorbing and reflecting properties of boundaries in acoustics are often defined as normalised quantities related to the loss in energy when a portion of the material is tested under conditions such as energy loss time when placed in a reverberation chamber [15]. The equation to calculate acoustic impedance based on absorption coefficient is as follows:

$$z = \rho c \frac{1 + \sqrt{1-a}}{1 - \sqrt{1-a}} \quad (3.7)$$

Due to the spatially staggered grids in FDTD, it is possible to handle the outer boundaries of a rectilinear domain in the velocity components by increasing the size of the velocity matrices by 1 in the direction of the velocity i.e. the length of a 3 dimensional u_x matrix would be:

$$u_{x,y,z} = (x = N+1, y = N, z = N) \quad (3.8)$$

Where the size of the p matrix is:

$$p_{x,y,z} = N : N : N.$$

For convenience and simplicity, local constant terms for the boundary can be lumped into an R parameter:

$$R = \frac{\rho \delta x}{0.5 \delta t} \quad (3.9)$$

This parameter reflects the handling of the boundary differential only being a half-step in time. Rearranging the form of the velocity equation to include a the partial derivative acoustic impedance component at the negative x boundary can be given as follows:

$$u_x^{t+\frac{\delta t}{2}} = \frac{R-Z}{R+Z} u_x^{t-\frac{\delta t}{2}} - \frac{2}{R+Z} p_{x+\frac{\delta x}{2}}^t \quad (3.10)$$

In this implementation of the FDTD method no internal obstacles are handled. In the study by Angus *et al* [21], obstacles were handled simply by setting local velocity values to 0 imposing a totally hard boundary within the domain. An improvement to this may be to implement the absorbing boundary conditions discussed above to the outside velocity points of an obstacle, allowing the obstacles to partially absorb.

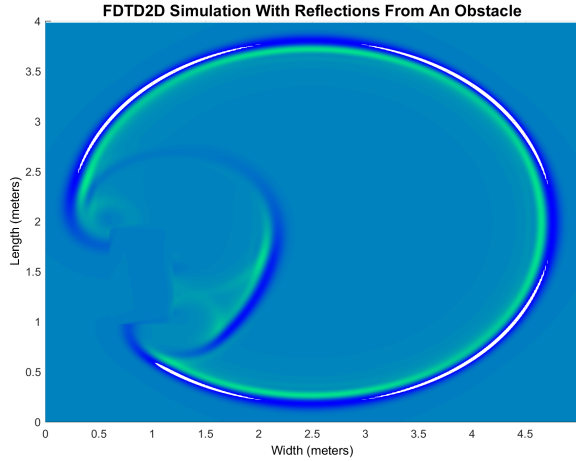
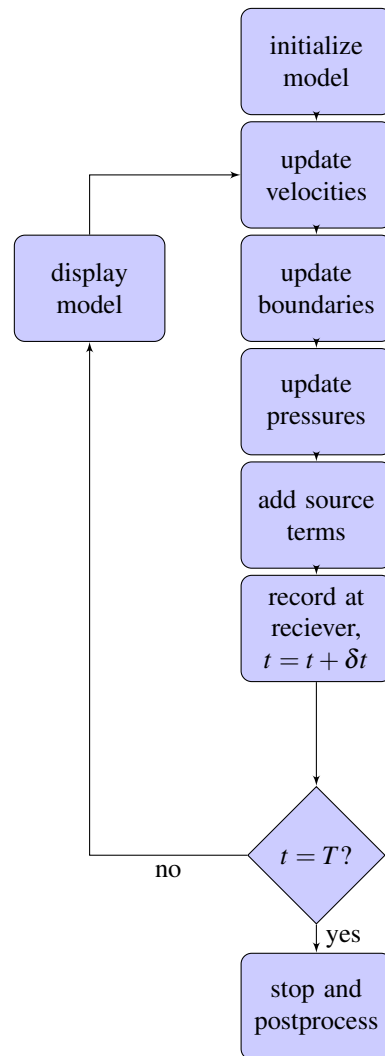


Figure 3.3: Example Plot of an FDTD Simulation With Reflection From an Obstable

3.1.5 Block Diagram

A basic block diagram of a program for solving the the acoustic FDTD method is given bellow:



3.1.6 Example Update Function

Below, is a function written in the Matlab language that is written to solve one time step of the wave equation using the FDTD method in 3 dimensions:

```

1 function [p, ux, uy, uz] = FDTD3Dfun(p, pCx, pCy, pCz, ux, uy, uz, uCx
2     ...
3     uCy, uCz, Rx, Ry, Rz, ZxN, ZxP, ZyN, ZyP, ZzN, ZzP)
4 % Function that performs one timestep of FDTD method for acoustic
5 % simulation.
6 %
7 % This function performs central finite difference calculations on
8 % matrices that represent pressure and velocity. This function assumes
9 % that a linear acoustic wave equation is being solved, and so assumes
10 % that
11 % the velocity terms are orthogonal and there are no cross-terms. This
12 % function solves empirical semi-absorbing boundary conditions, using
13 % the
14 % acoustic impedance of the boundary based on a normalised approximation
15 % of
16 % absorption coefficient.
17 %
18 % Takes the following arguments:
19 % p = N:N:N matrix of pressure values
20 % ux = N:N+1:N matrix of velocity values
21 % uy = N+1:N:N matrix of velocity values
22 % uz = N:N:N+1 matrix of velocity values
23 % pCx = constant related to pressure calculation in x direction
24 % pCy = constant related to pressure calculation in y direction
25 % pCz = constant related to pressure calculation in z direction
26 % uCx = constant related to velocity calculation in x direction
27 % uCy = constant related to velocity calculation in y direction
28 % uCz = constant related to velocity calculation in z direction
29 % Rx = (rho0*dx)/(0.5*dt) Constant related to field constants
30 % Ry = (rho0*dy)/(0.5*dt) Constant related to field constants
31 % Rz = (rho0*dz)/(0.5*dt) Constant related to field constants
32 % ZxN = acoustics impedance term at boundary in -x direction
33 % ZxP = acoustics impedance term at boundary in +x direction
34 % ZyN = acoustics impedance term at boundary in -y direction
35 % ZyP = acoustics impedance term at boundary in +y direction
36 % ZzN = acoustics impedance term at boundary in -z direction
37 % ZzP = acoustics impedance term at boundary in +z direction
38 %
39 % This function returns the pressure and velocity field matrices
40 %
41 % Calculate central difference approximation to velocity field
42 % Velocity in a direction at current timestep excluding the
43 % boundaries
44 % = velocity 1 time step ago - constants * pressure
45 % differential half a time step ago in that direction
46 ux(:, 2:end-1, :) = ux(:, 2:end-1,:) - uCx*(p(:, 2:end,:)) - p(:, 1:
47 end-1, :));
48 uy(2:end-1, :, :) = uy(2:end-1, :, :) - uCy*(p(2:end, :, :)) - p(1:
49 end-1, :, :));
50 uz(:, :, 2:end-1) = uz(:, :, 2:end-1) - uCz*(p(:, :, 2:end)) - p(:, :
51 1:end-1));

```

```

45 % update the velocity at the negative x boundary
46 % Velocity at this boundary for all of y and z = time and space
47 step
48 % normalised by the lovel impedance condition * current velocity
49 values
50 % - 2 / time and space discretization * local pressure value
51 ux(:, 1, :) = ((Rx - ZxN)/(Rx + ZxN))*ux(:, 1, :) ...
52 - (2/(Rx + ZxN))*p(:, 1, :);

53 % update the velocity at the positive x boundary
54 ux(:, end, :) = ((Rx - ZxP)/(Rx + ZxP))*ux(:, end, :) ...
55 + (2/(Rx + ZxP))*p(:, end, :);

56 % update the velocity at the negative y boundary
57 uy(1, :, :) = ((Ry - ZyN)/(Ry + ZyN))*uy(1, :, :) ...
58 - (2/(Ry + ZyN))*p(1, :, :);

59 % update the velocity at the positive y boundary
60 uy(end, :, :) = ((Ry - ZyP)/(Ry + ZyP))*uy(end, :, :) ...
61 + (2/(Ry + ZyP))*p(end, :, :);

62 % update the velocity at the negative z boundary
63 uz(:, :, 1) = ((Rz - ZzN)/(Rz + ZzN))*uz(:, :, 1) ...
64 - (2/(Rz + ZzN))*p(:, :, 1);

65 % update the velocity at the positive z boundary
66 uz(:, :, end) = ((Rz - ZzP)/(Rz + ZzP))*uz(:, :, end) ...
67 + (2/(Rz + ZzP))*p(:, :, end);

68 % update the pressure at all nodes
69 % new pressure across domain = pressure across domain 1 time step
70 ago -
71 % (space ,time and wave speed constant) * central difference of
72 % velocities half a time step ago in all three dimensions
73 p = p - pCx*(ux(:, 2:end, :) - ux(:, 1:end-1, :)) ...
74 - pCy*(uy(2:end, :, :) - uy(1:end-1, :, :)) ...
75 - pCz*(uz(:, :, 2:end) - uz(:, :, 1:end-1));
76
77 end

```

3.1.7 Stability

Surrounding this formulation of the FDTD method for the acoustic wave equation, it may be important to ensure appropriate conditions are met for a converging and stable solution. As this is an explicit time marching method, the Courant-Friedrichs-Lowy (CFL) stability condition may provide a guide for generating appropriate spatial and temporal discretisation steps [4, 17, 21–23]. The CFL condition implies that spatial δx and temporal δt discretization of a wave propagation model must be sufficiently small, that a single step in time is equal to or smaller than the time required for a wave to cross a spatial discretization step. This concerns both the speed of wave propagation c , the number of dimensions N_D and maximum simulation frequency f_{max} . The 2 dimensional CFL condition can be computed as such, where the CFL limit C_{max} is approximately 1 due to the use of an explicit time stepping solver:

$$CFL = c \frac{\delta t}{\sqrt{\sum_1^{N_D} \delta N_D^2}} \leq C_{max} \quad (3.11)$$

As the number of dimensions increases and the spatial step decreases, the time step must decrease for the simulation to remain stable. Although a simulation must have a CFL coefficient that is less than the C_{max} , this does not guarantee numerical stability and there is a lower limit of time step that can be observed in a poorly defined simulation.

As this acoustic simulation is a discrete computation of a continuous system, the Nyquist sampling theorem must be considered. This suggests that $\delta t \leq \frac{f_{max}}{2}$. It has been suggested in various studies [4, 24] that between 5 and 10 points per shortest wavelength are required for accurate stable simulation $\delta_x = c/(f_{max}6)$. As δx and δt are linked by the CFL condition, $\delta t \leq \frac{\frac{1}{c}\delta_x}{2}$. Stability analysis techniques are available for analysing the stability of simply shaped unbounded models such as VonNeuman analysis [23, 25]. Due to time constraints VonNeuman Analysis was not implemented in this study.

3.2 Sparse FDTD

3.2.1 Introduction to the Sparse Finite Difference Time Domain Method

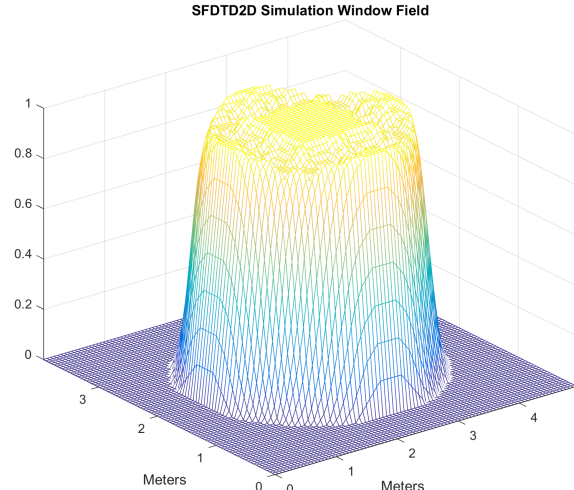
The sparse FDTD method (SFDTD) is a variant of the FDTD method proposed by Doerr [26] for use in the modelling of optical problems with significantly large domains such as PIC micro-controllers. Doerr has a patent on the application of the SFDTD method for computational electromagnetics [27]. This is not to be confused with sparse matrix solvers used for decomposing large sparse matrices in implicit FDTD methods. The SFDTD method relies on setting an appropriate threshold, and uses this threshold to determine points in the simulation domain that should be solved and points that should be ignored. This is analogous to applying a gate or window to the domain being computed, where ignoring parts of the domain with sufficient energy may significantly reduce computation time.

The approach suggested by Doerr is similar to the moving window FDTD method implemented by Schuster *et al* [28], in that the number of computations undertaken at any one time is significantly reduced and may improve computation time in a large simulation. However unlike moving window FDTD, the SFDTD implementation suggested by Doerr dynamically accommodates high and low energy points as the simulation continues. This is achieved by maintaining a set of lists of currently active points, previously active points and a matrix that parallels the domain and contains list indices. Doerr's method relies on constantly maintaining lists, and a pointing array that is the same size as the domain.

Maintaining multiple large lists in memory may be detrimental to the speed of execution in a large system where non-contiguous memory accesses are expensive in time. This may be of further concern when considering the difference in behaviour between electromagnetic and acoustics waves. Electromagnetic waves are transverse and can travel through a vacuum, acoustic waves are longitudinal and mechanical i.e. are fluctuations in a medium. Mechanical waves diffuse but photons in a PIC simulation may not, and the addressing of multiple lists with diffusing mechanical waves may be less practical than in PIC simulations. As such another method of windowing is explored below.

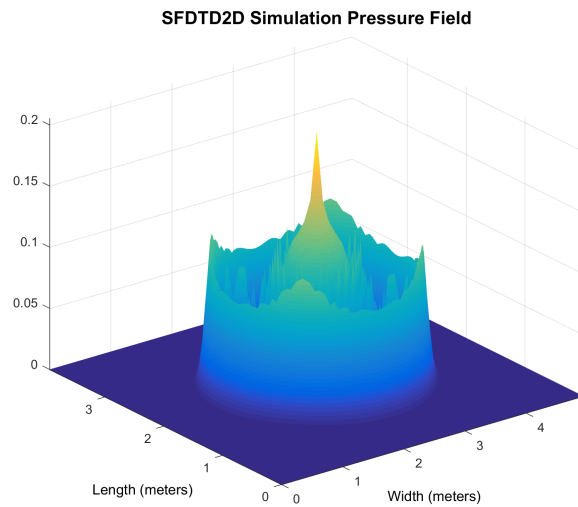
3.2.2 Acoustic Implementation of SFDTD in Two Dimensions

The implementation of the SFDTD for 2D simulation in this study attempts to leverage some signal processing techniques instead of search algorithms or individual checks like Doerrs method. The aim of is to generate a single indexing matrix as opposed to having an indexing matrix and lists. The points of the matrix will be used as a mask, where points with an absolute pressure above a threshold and surrounding points will be computed. The figure below shows the window shape and function shape for an SFDTD simulation at the same point in time.



(a)
b

Figure 3.4: Window Function



(a)
b

Figure 3.5: Pressure Function

Figure 3.6: Caption place holder

Figure 3.7: Examples of an Expanding Wave in an SFDTD Simulation

The domains of interest in this study are large and contain many points. To generate index points around those with adequate pressure to be calculated, some smoothing of the pressures in the matrix is required. This could be thought of as similar to a blurring effect or smoothing in image processing [29], which is the process of convolving an image with a Gaussian function and essentially low-pass filtering the image. This process reduces noise and details of an image, and thus should smooth around the threshold window and allow the processing mask in the SFDTD method to work just outside of the confines of the areas where the pressure is above the threshold. Below is a Matlab function for calculating such a matrix:

```

1 function [ idx ] = SPARSEfun2DC(p, thresholddB , p0)
2 %Transform threshold to Pa
3 threshold = p0 * 10^(thresholddB/20);
4 %Calculate blurring filter
5 PSF = fspecial('gaussian',7,10);
6 %Create copy of p that is normalised by threshold
7 temp = abs(p) ./ threshold;
8 %Set the 'quiet' regions to 0
9 temp2 = floor(temp);
10 %Reduce values above 1 to 1, so that blurring isn't too strong in some
11 areas
11 temp2(temp2 > 1) = 1;
12 %Convolve 2d matrix with gaussian blurring filter to smooth
13 idx = imfilter(temp2,PSF,'symmetric','conv');
14 end
```

Below is an example surf plot of the window matrix for a 50m by 40m simulation with a maximum sampling frequency of 1kHz and a windows threshold of 40dB.

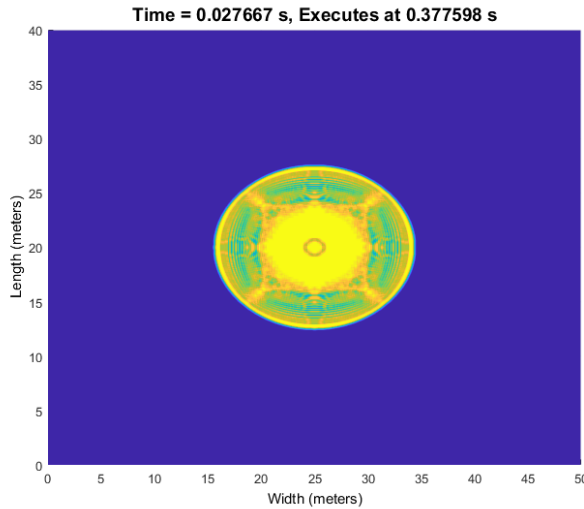


Figure 3.8: Window of an expanding wave in an SFDTD simulation

It can be seen that the dispersion error caused by the rectilinear system is imprinted on the window. Dispersion error is the phase error with which different frequencies travel in an FDTD simulation [30], and low order staggered schemes may suffer considerably from this error. There is ongoing research as to the perceptual effects of dispersion error in different FDTD schemes, when calculating impulse responses for auralization. Further experimentation using a higher order FDTD scheme may reduce numerical dispersion [24, 25] and improve the effectiveness of the window in reducing computation area to wave-fronts.

The figure below shows the window shape for a similar simulation to the one above, but with a threshold of 60dB.

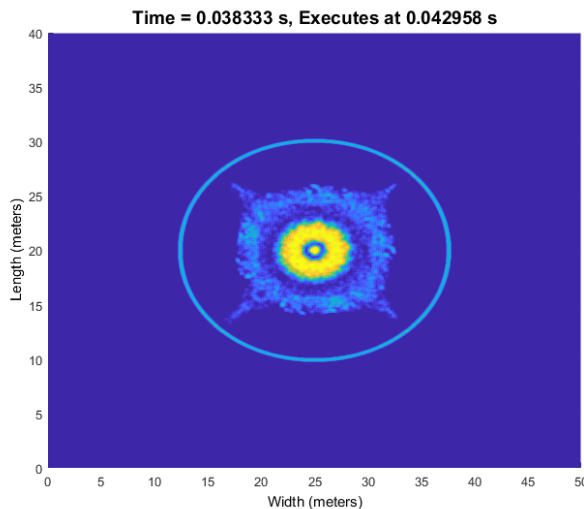


Figure 3.9: Window of an expanding wave in an SFDTD simulation

It can be seen that the dispersion trailing the outer wave-front has been truncated. This is reflected in the figure below that shows the power spectrum for a receiver 12m away from the sound source for three simulations. This suggests that the SFDTD methods is essentially reducing the level of the spectrum, and is reducing the signal to noise ratio. Below is a plot of the execution speed of time steps as the same simulations progress, for a number of thresholds:

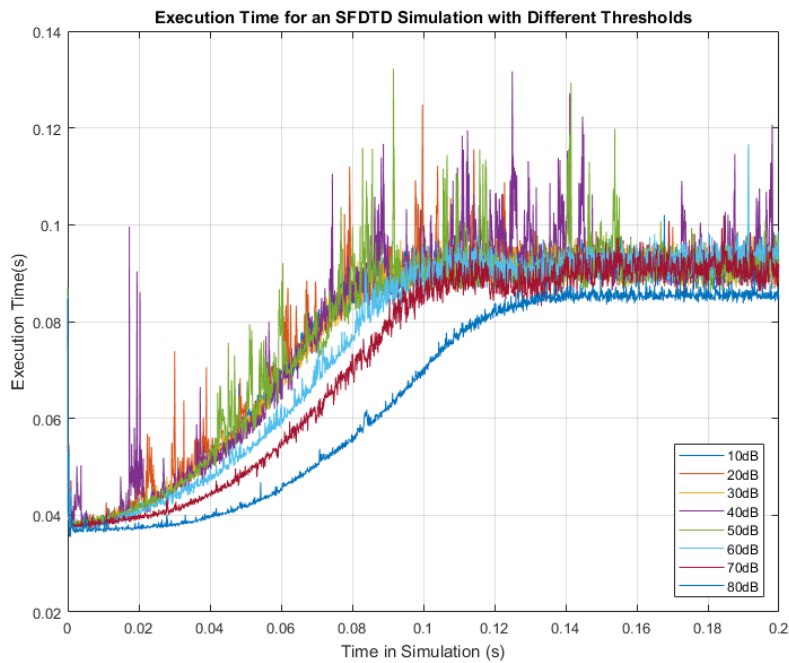


Figure 3.10: Smoothed rate of time step execution for the SFDTD method during simulations, for different threshold levels

The figure below shows that simulations in small domains using the SFDTD method can still exhibit traditional wave patterns:

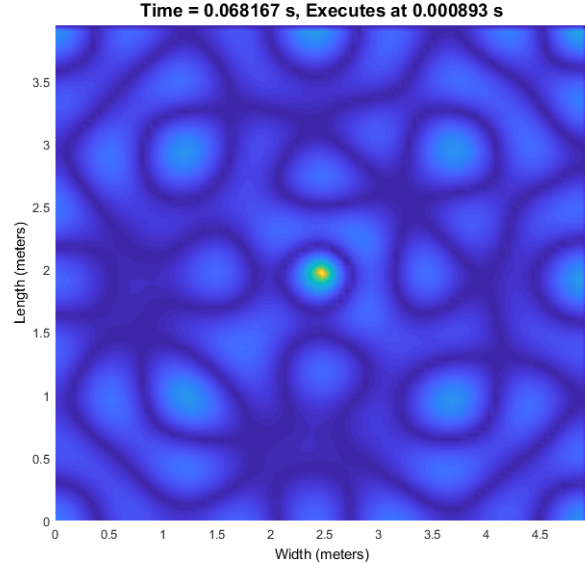


Figure 3.11: Single source SFDTD simulation in a small room with nodes and anti-nodes present

It can be seen that increasing the threshold level of the windowing function decreases aggregate and individual execution times, and begins to become much faster with a threshold above 40dB. The FDTD algorithm above is adjusted to reference this matrix and operate at non-zero coordinates, calculating not only the regions with appropriate amounts of power but also the surrounding cells. The current implementation uses an if statement which is potentially very slow, and would not be easy to solve in parallel arithmetically. As well as implementing this method in 3D, it may be crucial to develop a method for masking the simulation and solving without using any if statements. Depending on the simulation, the level of the threshold value may be set as a single value or may be set to decrease over time to accommodate diffuse field calculation. However if an appropriate lossy wave equation was implemented, it may be possible to use a relatively high threshold to compute propagation loss for wave-fronts such as strong and early reflections.

3.3 Pseudo-Spectral Time Domain Method

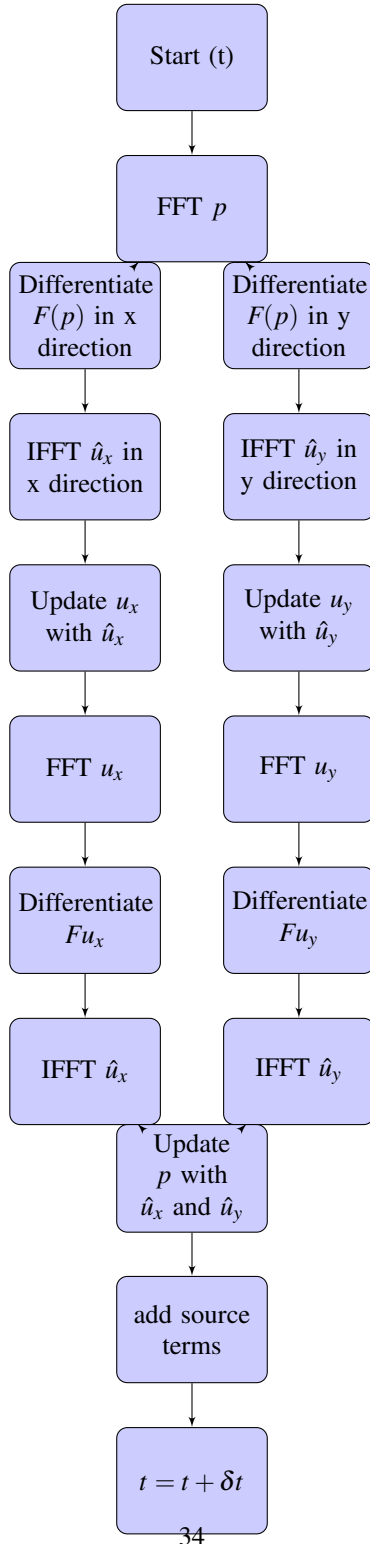
The Fourier Pseudo-spectral Time Domain (PSTD) Method is a numerical method that can be used for solving partial differential equations in a similar way to the FDTD method. The advantage of this method is that differentiation occurs in the frequency domain, using the computational speed of performing a discrete Fourier transform to give fast frequency domain differentiation and differentiation with higher order accuracy than the FDTD method [31]. In this chapter we will discuss the application of the PSTD method to the acoustic wave equation, including the use of empirical partially absorbing boundary conditions and the perfectly matched layer(PML).

3.3.1 A Background to the Pseudo-Spectral Time Domain Method

The PSTD method is of a branch of spectral methods that are useful for solving some hyperbolic partial differential equations. Use of spectral differentiation for computational fluid dynamics modelling was first proposed by Orszag [32], and was further expanded by Kriess and Oliger [33]. Fourier Pseudospectral methods have been advanced considerably since then, and have found applications in weather prediction, particle physics, electromagnetics and acoustics. More recently Trefethen [34] presented a classic text showcasing both the power of spectral methods, and how simply they could be implemented. The Fourier PSTD method used in this study is advanced from that presented by Angus and Caunce [21], with expansion into 2 and 3 dimensions and implementation of partially absorbing boundary conditions.

3.3.2 Block Diagram

The basic block diagram of a program for solving the the acoustic PSTD method is very similar to the FDTD Method. Below is a block diagram of the steps for solving one time step of the 2D PSTD method:



3.3.3 The Pseudospectral Time Domain Method Applied To The Wave Equation

The acoustic wave equation has been previously defined with two resolving parts:

$$\frac{\delta^2 p}{\delta t^2} = \frac{1}{c^2} \frac{\delta^2 p}{\delta t^2} \quad (3.12)$$

$$\frac{\delta^2 u}{\delta t^2} = \frac{1}{c^2} \frac{\delta^2 u}{\delta t^2} \quad (3.13)$$

Applying a continuous time Euler solving method to the above relationship with respect to space brings the following:

$$\rho_0 \frac{\delta}{\delta x} \left[\frac{\delta u}{\delta t} \right] = \frac{1}{c^2} \frac{\delta^2 p}{\delta t^2} \quad (3.14)$$

Implementing a discrete time and space version of this equation using an FDTD scheme yields:

$$u_x^{t+\frac{\delta t}{2}} = u_x^{t-\frac{\delta t}{2}} - \frac{\delta t}{\rho \delta x} \left[p_{x+\frac{\delta x}{2}}^t - p_{x-\frac{\delta x}{2}}^t \right] \quad (3.15)$$

$$p_x^{t+\frac{\delta t}{2}} = p_x^{t-\frac{\delta t}{2}} - \frac{c^2 \rho \delta t}{\delta x} \left[u_{x+\frac{\delta x}{2}}^t - u_{x-\frac{\delta x}{2}}^t \right] \quad (3.16)$$

The PSTD method applies differentiation in the frequency or *k*space domain. This can be represented as:

$$u_x^{t+\frac{\delta t}{2}} = u_x^{t-\frac{\delta t}{2}} - \frac{\delta t}{\rho \delta x} \mathbf{F}^{-1} (\varepsilon \mathbf{F} [p_x^t]) \quad (3.17)$$

$$p_x^{t+\frac{\delta t}{2}} = p_x^{t-\frac{\delta t}{2}} - \frac{c^2 \rho \delta t}{\delta x} \mathbf{F}^{-1} (\varepsilon \mathbf{F} [u_x^t]) \quad (3.18)$$

Where \mathbf{F} represents the forward and \mathbf{F}^{-1} the inverse Fourier Transforms respectively, and ε is a differentiating function representing:

$$\mathbf{J}\mathbf{K}_N \exp^{-jk_N \frac{\delta x}{2}} \quad (3.19)$$

Which is the impulse response of a differentiating function in the complex domain, where N is the 1D size of the domain in the dimension of interest i.e. each dimension requires a differentiator function. In the 2D and 3D implementation of this method, extra velocity terms are added to handle the differentiation of directionally dependent terms:

$$u_x^{t+\frac{\delta t}{2}} = u_x^{t-\frac{\delta t}{2}} - \frac{\delta t}{\rho \delta x} \mathbf{F}^{-1} (\varepsilon \mathbf{F} [p_x^t]) \quad (3.20)$$

$$u_y^{t+\frac{\delta t}{2}} = u_y^{t-\frac{\delta t}{2}} - \frac{\delta t}{\rho \delta y} \mathbf{F}^{-1} (\varepsilon \mathbf{F} [p_y^t]) \quad (3.21)$$

$$u_z^{t+\frac{\delta t}{2}} = u_z^{t-\frac{\delta t}{2}} - \frac{\delta t}{\rho \delta z} \mathbf{F}^{-1} (\boldsymbol{\varepsilon} \mathbf{F} [p_z^t]) \quad (3.22)$$

$$p_{xyz}^{t+\frac{\delta t}{2}} = p_{xyz}^{t-\frac{\delta t}{2}} - \frac{c^2 \rho \delta t}{\delta x} \mathbf{F}^{-1} (\boldsymbol{\varepsilon} \mathbf{F} [u_x^t]) - \frac{c^2 \rho \delta t}{\delta y} \mathbf{F}^{-1} (\boldsymbol{\varepsilon} \mathbf{F} [u_y^t]) - \frac{c^2 \rho \delta t}{\delta z} \mathbf{F}^{-1} (\boldsymbol{\varepsilon} \mathbf{F} [u_z^t]) \quad (3.23)$$

The figure below shows a 2D matrix used for differentiation on a 2D simulation in one direction:

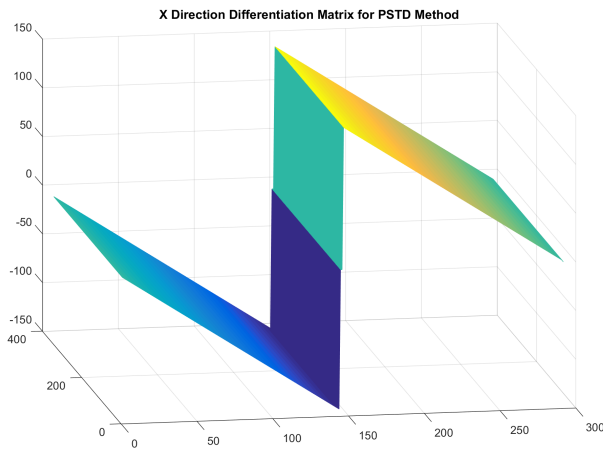


Figure 3.12: 2D Differentiation Matrix in 1 Direction for a PSTD Simulation

A Matlab function for solving 1 time step of the PSTD method is given below:

```

1 %%%%%%
2 % PTSD3Dfun.m
3 % Created by S Durbridge as part of work on a masters dissertation
4 % Copywrite S Durbridge 2017
5 %
6 % Any copies of this function distributed by the autor are done so
7 % without any form of warranty , and should not be reproduced without
8 % permission
9 %%%%%%
10
11 function [pd, udx, udy, udz] = PTSD3Dfun(pd, udx, udy, udz ,...
12 diffmatrixX , diffmatrixY , diffmatrixZ ,...
13 PMLdiff, PMLalphau, PMLalphap, PMLconst)
14 %% Function solves using the PSTD method for a pressure vector ,...
15 % velocity vector and differentiation impulse response in 1
16 % dimension
17 % and returns the solved pressure and velocity vectors
18
19 %% Velocity in 3d
phat = fftn(pd);

```

```

20 temp1 = phat .* diffmatrixX;
21 temp2 = phat .* diffmatrixY;
22 temp3 = phat .* diffmatrixZ;
23
24 pdiffhatx = ifftn(temp1, 'symmetric');
25 pdiffhaty = ifftn(temp2, 'symmetric');
26 pdiffhatz = ifftn(temp3, 'symmetric');
27
28 %% Total Velocity
29 udx = udx .* PMLdiff - PMLalphau .* (pdiffhatx ./ PMLconst);
30 udy = udy .* PMLdiff - PMLalphau .* (pdiffhaty ./ PMLconst);
31 udz = udz .* PMLdiff - PMLalphau .* (pdiffhatz ./ PMLconst);
32
33 %% Pressure in 3d
34 uhat = fftn(udx);
35 temp = uhat .* diffmatrixX;
36 udifffhatx = ifftn(temp, 'symmetric');
37
38 %% Pressure in 3d
39 uhat = fftn(udy);
40 temp = uhat .* diffmatrixY;
41 udifffhaty = ifftn(temp, 'symmetric');
42
43 %% Pressure in 3d
44 uhat = fftn(udz);
45 temp = uhat .* diffmatrixZ;
46 udifffhatz = ifftn(temp, 'symmetric');
47
48 %% Total Pressure
49 pd = pd .* PMLdiff - (PMLalphap .* (udifffhatx ./ (PMLconst))) ...
50 - (PMLalphap .* (udifffhaty ./ (PMLconst))) ...
51 - (PMLalphap .* (udifffhatz ./ (PMLconst)));
52
53 end

```

3.3.4 Absorbing Boundary Conditions

The Fourier PSTD is performs well for problems with smoothly varying properties, but this method suffers from Gibbs phenomenon as the domain is periodic and has discontinuity at its boundaries i.e. it is not infinitely long. This is manifested as aliasing in the domain. A way to reduce this aliasing is to increase the area of the domain and implement a perfectly matched layer (PML). A PML is a totally absorbing boundary condition that absorbs waves travelling into it without causing reflection due to impedance mismatching, as opposed to a more simple boundary condition such as Dirichlet (fixed) that will cause reflections [35]. The PML was first developed for Maxwell's Equations in Computational Electromagnetics by Berenger [36], and was quickly developed for other applications such as acoustic FDTD and FE [37].

Three predominant types of PML available are the split field PML, Uniaxial PML and the Convolutional PML. For the sake of time saving and simplicity, the uniaxial PML is implemented in this study as is implemented in the source literature [21]. The PML is implemented as a matrix with the same dimensions as the domain, which has

been extended in each dimension by the number of cells matching the desired depth of the PML N_{pml} . In the PML region, the value of the PML contribution to the p and u update equations σ , reduces in value from 1 to 0 towards the final boundary of the domain, continuously and smoothly impeding acoustic waves in any direction within the PML causing no reflection of waves from the PML back into the domain main domain.

The modified 1D update equation for this is as follows:

$$u_x^{t+\frac{\delta t}{2}} = u_x^{t-\frac{\delta t}{2}} \sigma_a - \frac{\delta t}{\rho \delta x} \sigma_b \mathbf{F}^{-1} (\varepsilon \mathbf{F} [p^t]) \quad (3.24)$$

$$p_x^{t+\frac{\delta t}{2}} = p_x^{t-\frac{\delta t}{2}} \sigma_a - \frac{c^2 \rho \delta t}{\delta x} \sigma_b \mathbf{F}^{-1} (\varepsilon \mathbf{F} [u^t]) \quad (3.25)$$

Where:

$$\begin{aligned} \sigma_a &= \frac{1-a}{1+a} \\ \sigma_b &= \frac{1}{1+a} \\ d &= PMLDepth \\ N &= TotalArrayLength \\ i &= 1, 2, \dots, N-1 \\ i < d \quad a &= \frac{1}{3} \left(\frac{i}{d} \right)^3 \\ d < i < N-d \quad a &= 0 \\ i > N-d \quad a &= \frac{1}{2} \left(\frac{N-i}{d} \right)^3 \end{aligned} \quad (3.26)$$

As the maximum number in the matrix is 1, a multidimensional implementation of the PML regions involved creating orthogonal arrays of these 1D sections and applying an average summation of the regions values. Generating 2D PML coefficients involves summing 2 orthogonal 2D $N_x N_y$ matrices using a least squares method. Generating a 3D matrix of PML coefficients involved creating 3 3D $N_x N_y N_z$ matrices, with sets of 1D coefficient arrays in each direction. These three orthogonal matrices are summed and divided by the number of matrices. An example of the values of PML coefficients in a 2D simulation can be found below:

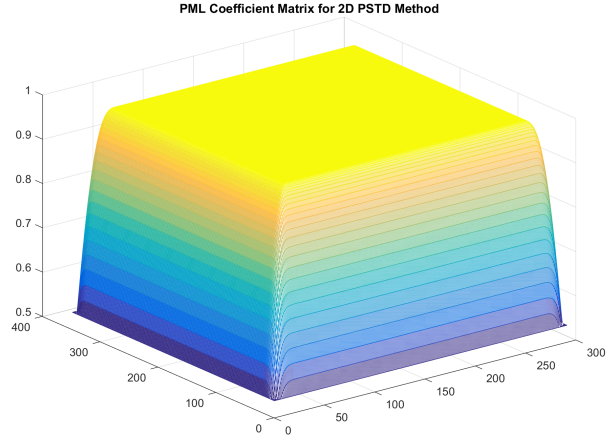


Figure 3.13: PSTD 2D PML Coefficient Matrix

3.3.5 Partially Absorbing Boundary Conditions

Partially absorbing boundary conditions for PSTD are implemented in this study using the methods explored by Spa *et al.* [38], where a real and normalised value can be defined and used as a frequency independent absorption coefficient for boundary impedance setting. This method applies a weighting to the relationship between pressure and velocity at the grid boundaries, reflecting and passing a proportion of energy.

This boundary handling method uses the principal of acoustic impedance Z mentioned previously, to absorb or reflect at the imposed boundary of the domain. The relationship between boundary coefficient ξ , and acoustic impedance is as follows:

$$\begin{aligned}
 & \text{For } \xi \leq 1 : \\
 \xi &= \frac{Z/(\rho c)}{S + Z/(\rho c) - ZS/(\rho c)} \\
 & \text{For } \xi \geq 1 : \\
 \xi &= ZS/(\rho c) - S + 1
 \end{aligned} \tag{3.27}$$

Where S is the CFL coefficient of the simulation. As the boundary will present a discontinuity and cause aliasing, the PML will be included outside of the partially absorbing boundary to try and counteract the error. At the point where the partially absorbing boundary occurs, the scaling term ξ is set to either scale the p or u value depending on the value of ξ at that point. The value of ξ is determined by normalising the relationship between specified absorption value α , and S :

$$\begin{aligned}
S &= \frac{\delta t}{\delta x} \\
\xi_n &= 1 - \alpha \\
\xi &= \frac{(1 + \xi_n)}{(1 + \xi_n - 2 * S * \xi_n)}
\end{aligned} \tag{3.28}$$

The 1D update equations are then modified to handle ξ at the point of interest at the boundary of the domain:

$$\begin{aligned}
\text{For } \xi \leq 1 : \\
p_x^{t+\frac{\delta t}{2}} &= \xi \left[p_x^{t-\frac{\delta t}{2}} \sigma_a - \frac{c^2 \rho \delta t}{\delta x} \sigma_b \mathbf{F}^{-1} (\varepsilon \mathbf{F} [u^t]) \right] \\
\text{For } \xi \geq 1 : \\
u_x^{t+\frac{\delta t}{2}} &= \frac{1}{\xi} \left[u_x^{t-\frac{\delta t}{2}} \sigma_a - \frac{\delta t}{\rho \delta x} \sigma_b \mathbf{F}^{-1} (\varepsilon \mathbf{F} [p^t]) \right]
\end{aligned} \tag{3.29}$$

The figure below shows the pressure grid for a 2D PSTD simulation after some timesteps, including some reflections from a corner of the domain:

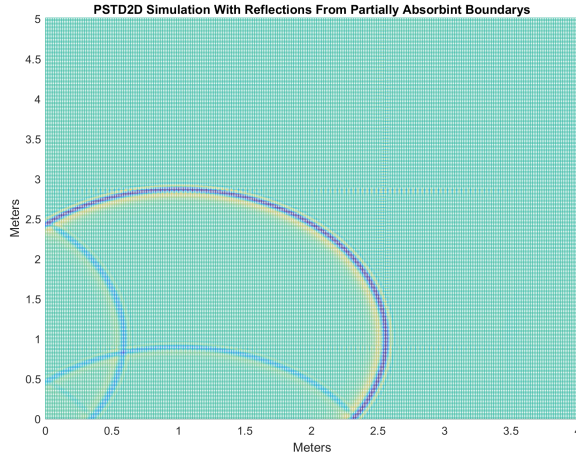


Figure 3.14: Example Plot of a 2D PSTD Simulation With Reflections

3.4 Sound Source Terms

There are three main sound source excitation strategies in FDTD and PSTD simulations; hard, soft and transparent sources [39]. Hard sources involve directly coupling a source signal to the pressure grid of a simulation, explicitly setting the pressure at a node for each time step of the simulation. This source type creates a discontinuity in

the domain, that itself will cause incoming waves to reflect and diffract around it. This method also causes a shift in the frequencies of modal artifacts [39]. A hard source maybe implemented using the following equation:

$$p_{xyz}^t = source^t \quad (3.30)$$

Where the source is a function of time and is evaluated at points of t up to T , and the points of p_{xyz} are the points of excitation of the domain. A soft source such as the one used in this study for all three methods, imposes a pressure perturbation term to the newly calculated pressure at the point of interest in the pressure grid. This allows waves to pass the source location without being impeded by the source term itself. A soft source can cause an anomalous DC term to be added to the simulation, causing a spectral shift to occur as seen in the power spectral density plots of this report. Also a soft source excitation may be modulated by the error present in the simulation grid, as the source term is indirectly coupled to the domain and is modulated by any passing waves. A soft source may be implemented using the following equation:

$$p_{xyz}^t = p_{xyz}' + source^t \quad (3.31)$$

A transparent source involves applying error correction to the stimulus by convolving the impulse response of the simulation pressure grid with the source signal being applied to the domain, and taking the error from the original signal. This should correct for the error caused by the discretization and solving scheme, and allow for an accurate soft source coupling i.e. without causing extra reflections. This method does however exhibit the same dc term and spectral tilt inherent in the soft source. The impulse response of the domain can be taken by recording the incoming pressure at the source excitation point, when the source term is an ideal dirac function. A transparent source can be implemented using the following equation:

$$p_{xyz}^t = p_{xyz}' + source^t - \sum_0^T h_{xyz}^{t=0:t} * source^{t=0:t} \quad (3.32)$$

Chapter 4

Validation

4.1 Validation Strategy

Model validation could be considered an important step towards creating a robust and useful simulation tool. A greater volume of literature is available for the validation of Ray based methods such as [40–42], and the validation of a hybrid scheme by Southern *et al* is available [43]. Studies such as Hill [4] incorporate validation as a subset of a greater work. This section will review the results of simulations using the FDTD and PSTD tools described above, with a small 3D domain and different excitation signals. The validation of these simulation tools will be in proving that wave propagation is occurring.

4.1.1 The Domain

The domain used was a fully bounded rectangular room with the following properties:

- Length $L_x = 5m$
- Width $L_y = 4m$
- Height $L_z = 3m$
- Volume $v = 60m^3$
- Surface Area $S_{area} = 94m^2$
- Uniform Absorption Coefficient $\alpha = 0.45$
- Schroeder Frequency $f_{schroeder} = 107Hz$,
- The Reflection Order $N_{reflections} = 30.7$
- Mean Free Path Between Reflections $MFP = 2.55m$

- Eyring Reverberation Time $RT_{60} = 0.1719s$

The theoretical room mode frequencies below the Schroeder frequency are shown below:

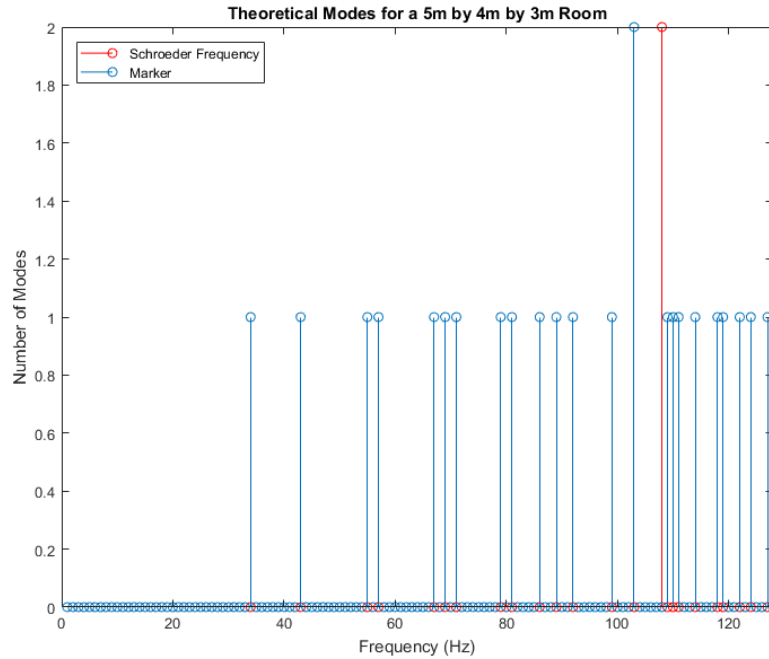


Figure 4.1: Room Modes up to Schroeder Frequency for a Small Rectangular Room

The source position was $1.0m$ in each direction from a bottom corner. Five receiver positions were recorded, one quarter on the x and y dimensions from each corner, all at the middle of the domain on the z axis. The source type was a soft source as described earlier in this document. Two source signals were implemented in separate simulations; an MLS sequence of 11th order with 2 repetitions, and a $1kHz$ tone burst signal containing three pulses of 10 cycles with a gap of equal length to the bursts. The MLS signal was generated using the MLS toolbox by Mark Thomas [44], and the tone-burst was generated using tools in the Matlab DSP Systems toolbox. The signals were normalised with a Gaussian window to the length of the signals. The maximum frequency of interest in this validation was $5kHz$, giving a $0.333e^{-5}$ step time for the FDTD and SFDTD simulation, and a $0.1e^{-4}$ step time for the PSTD simulation.

4.2 Results

The aim of the simulations was to show that the models propagate pressure waves with minimal error in the average power spectral density between source and receiver location. Frequency domain averaging of the source and receiver location signals was undertaken using Matlab pwelch function. This function uses Welch's overlapping segment averaging estimator to average a series of discrete Fourier transforms, creating a smoothed average frequency response over the course of the signal without transforming the whole signal in one go [?].

4.2.1 FDTD Simulation Results

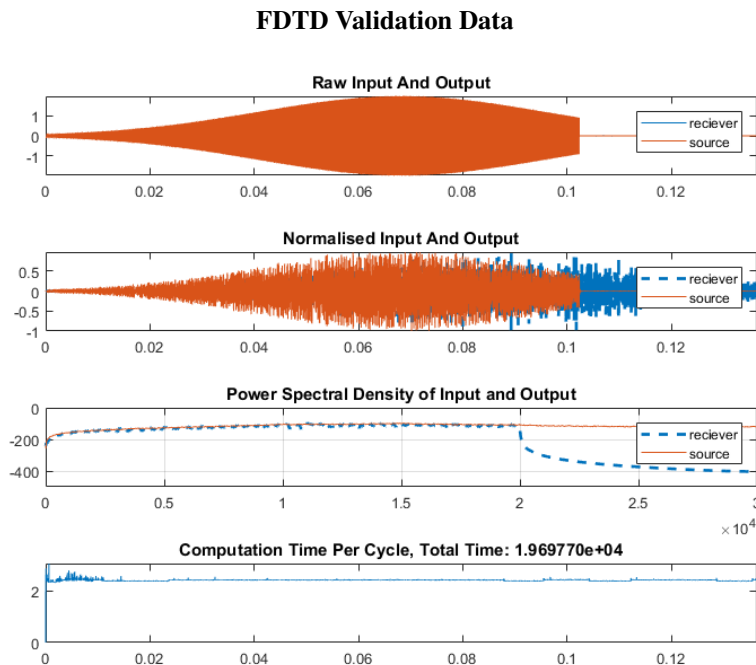


Figure 4.2: Validation data of FDTD simulation

4.2.2 SFDTD Simulation Results

Results

4.2.3 PSTD Simulation Results

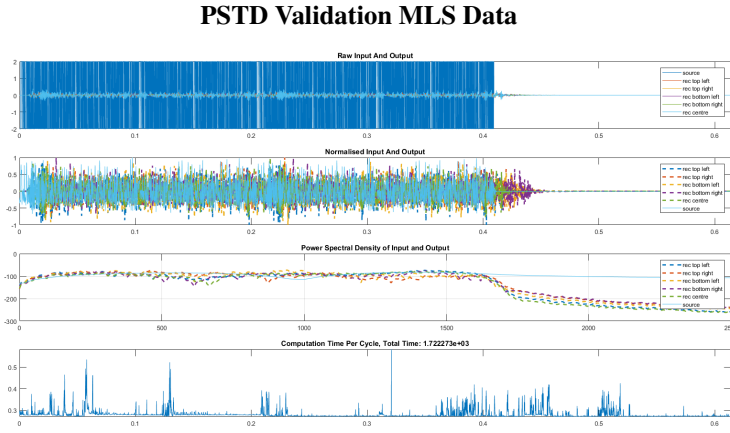


Figure 4.3: Validation data of PSTD simulation With MLS Source
PSTD Validation Tone Burst Data

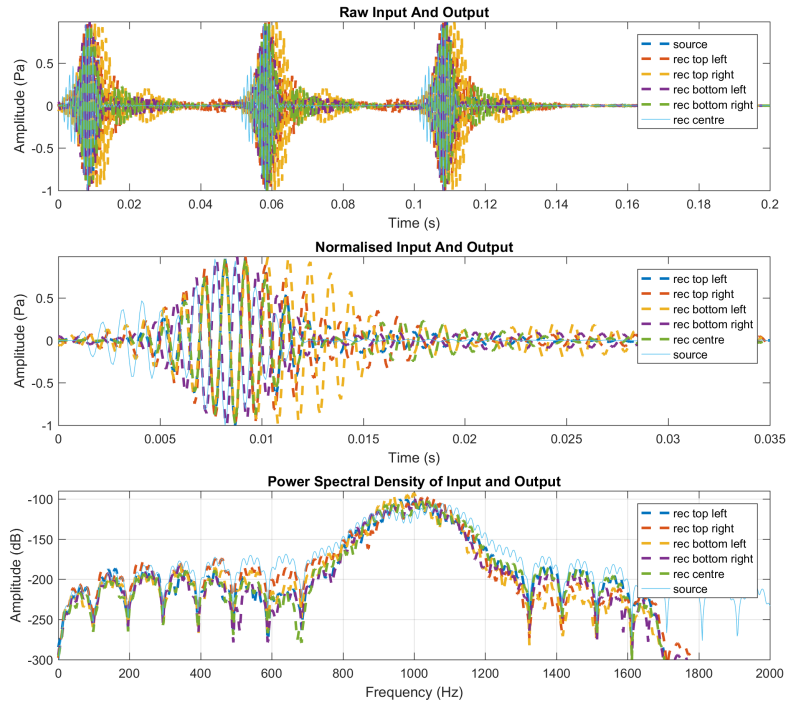


Figure 4.4: Validation data of PSTD simulation With Tone Burst Source

It can be seen that both simulations have reasonably good agreement between the power spectral densities (PSD) of the source and receivers in the frequency region of interest. There is a significant low frequency signal present in the PSTD response, in both the source and receiver sections. Due to the 6 steps per wavelength of the FDTD simulation, the time step was also smaller than for the PSTD simulation. As such when using Matlabs Welch function to perform PSD estimation, the estimation was made beyond the frequency range of interest.

4.3 Validating The SFDTD Method

As the SFDTD method was implemented only to 2D and it could not be validated with the 3D FDTD and PSTD methods as above. The SFDTD method was tested using a 5m by 4m domain, with absorption coefficients of $\alpha = 0.45$. The signal used was a chirp that was generated using the Chirp function of the Matlab DSP Systems Toolbox, with a start frequency of 100Hz and a stop frequency of half the maximum target frequency (or a quarter of Nyquist), that was normalised to 100dB SPL and has a sweep time of 0.4s. Before normalisation, a Hamming window was applied to the signal to minimize the discontinuity of introducing the source. The figure below presents the output data for the SFDTD validating simulation:

SFDTD Validation Data

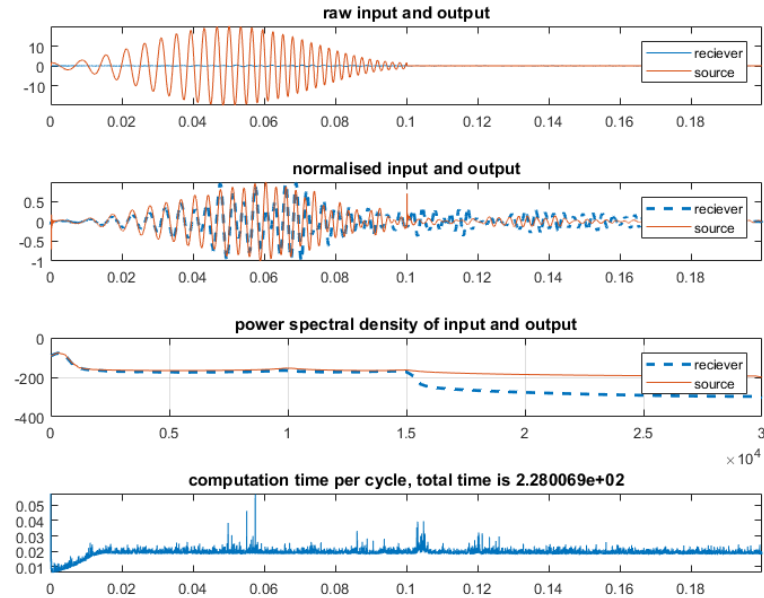


Figure 4.5: Validation data of PSTD simulation

As with the PSTD method there is a shared low frequency component, but the PSD between source and receiver are very close to well beyond the highest frequency of interest.

Chapter 5

Execution Time and Analysis

The interest of this study was to analyse the execution times of the three algorithms described above, to determine which method executes in the fastest time and thus might be most appropriate for using to solve large problems. The execution times were measured for each method for domains of the following sizes with a maximum frequency of 500Hz for FDTD and PSTD in 3D, and 1kHz for SFDTD in 2D:

Dimension (m^2)	FDTD Cells	SFDTDCells	PSTD Cells
5	121104	121104	24025
10	483025	483025	62500
20	1932100	1932100	192721
40	7722841	7722841	667489
60	30880249	30880249	2474329

The time step execution time was evaluated for 2000 executions, allowing for smaller or larger required time steps to be part of the analysis. The execution of each time step includes only the steps outlined above, with no plotting. Execution time was measured using Matlabs Tic and Toc functions. During execution, Matlab was the only task running in the foreground of the system, but background tasks were allowed to continue without restriction. The computer system used for these tests had the following properties:

- Intel Core i5 4690k CPU @ 4.5GHz @ 1.227V
- 16GB DDR3 RAM @ 3875.3MHz
- Asus Gryphon Motherboard with Z97 Chip Set

5.1 Results

The average execution time for each method is given below:

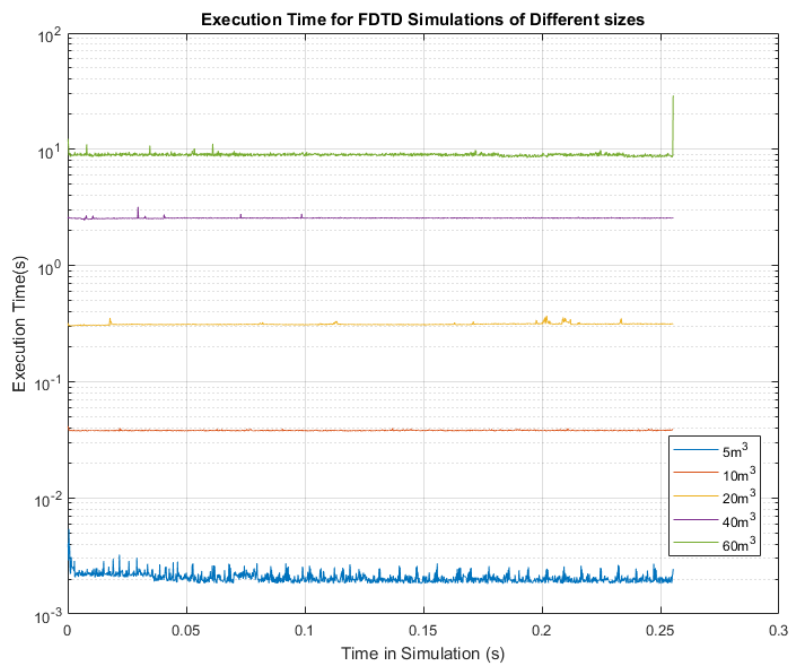


Figure 5.1: Execution times for FDTD simulations in domains of increasing size

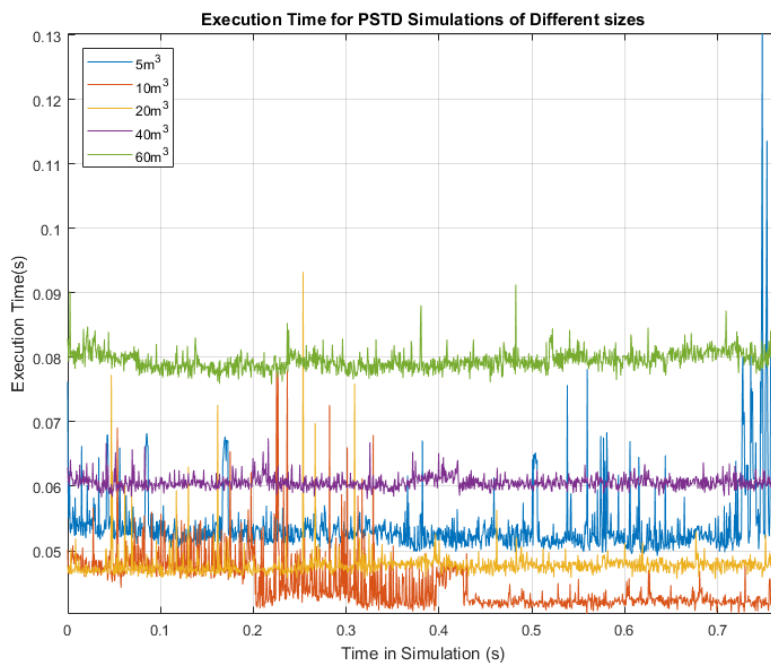


Figure 5.2: Execution times for PSTD simulations in domains of increasing size

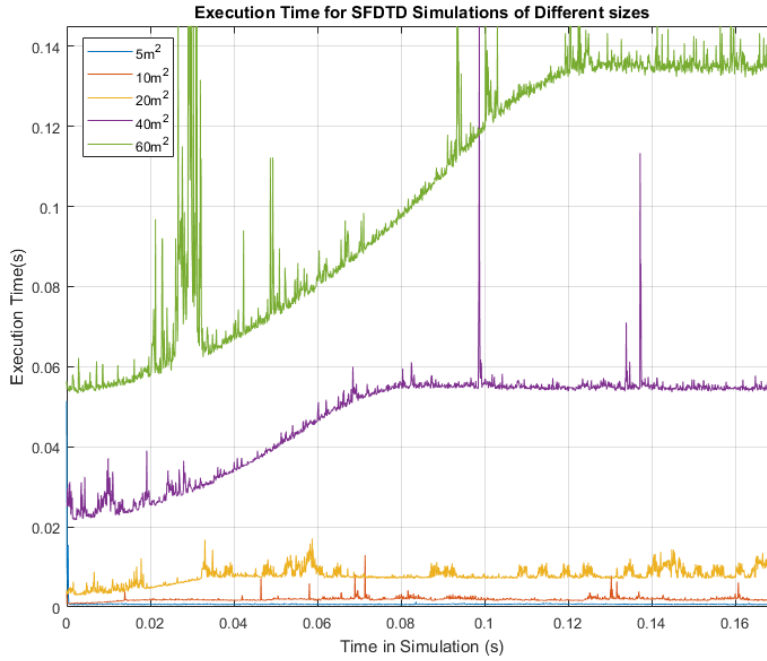


Figure 5.3: Execution times for SFDTD simulations in domains of increasing size

5.2 Analysis

These results show some interesting properties of simulation execution over time for the different methods. The FDTD method is significantly slower at executing than the PSTD and SFDTD methods, particularly with the larger domains. The aggregate execution time for 0.25s of simulation for a $40m^3$ domain was 1 hour 5 minutes. Whereas execution for the same domain in PSTD was 1.5 minutes. Execution time data for the PSTD method appears to fluctuate wildly compared to the FDTD data, and this is probably due to the influence of system loading by background tasks. These fluctuations are better masked by the log scaling in time for the plot of FDTD execution time data. This y axis scaling was chosen to give clearer reference to the range of execution times due to the size of each domain.

With this data, it is clear to see that the PSTD method executes significantly faster for larger domains than the FDTD method. This is likely due to three main reasons:

- Differentiation in the frequency domain allows large domains to be evaluated fast, as many cells are differentiated at once.

- The speed of the Fourier transforms is sufficiently fast to have little increase as the number of cells increases.
- Due to the nature of frequency domain differentiation, fewer cells are required per wavelength for stable simulation.

5.3 Code Profiling

Use of Matlabs code profiling tool analysis the performance of the PSTD3Dfun function shows the time taken for execution for 2000 calls of the function during an example simulation of a 5m by 4m by3m domain with a maximum frequency of 5kHz:

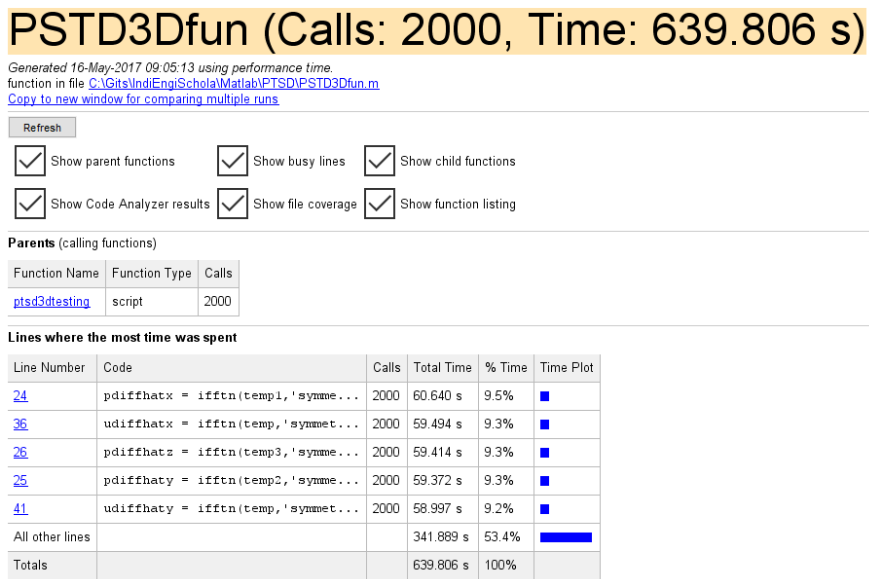


Figure 5.4: Code execution time profile of PSTD functions

This shows that most time in the execution was spent performing the IFFT of the 3D matrices, and that the maximum average differentiation time was 5.1ms for a matrix of 80724 points in the x direction. Below is a figure showing the code profiling for 1200 calls of the FDTD3Dfun function for an example simulation of a 5m by 4m by3m domain with a maximum frequency of 1kHz:

FDTD3Dfun (Calls: 1200, Time: 104.840 s)

Generated 16-May-2017 09:36:17 using performance time.
 function in file C:\Gits\ndl\EngSchola\Matlab\FDTD\FDTD3Dfun.m
[Copy to new window for comparing multiple runs](#)

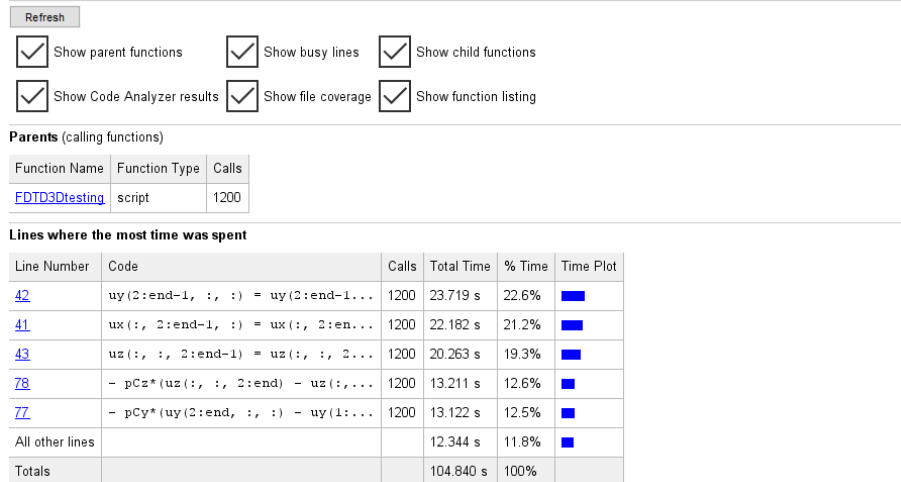


Figure 5.5: Code execution time profile of FDTD functions

These profiling results show that the bulk of the time spent in execution of the FDTD3Dfun function is used in the differentiation of the matrices. Combined with the total execution speed results for different domains above, the conclusion can be drawn that spectral differentiation may be more appropriate for large domains than finite or local differentiation. As the SFDTD method appears above to converge after some time to a uniform excution time, PSTD may be a more appropriate choice for further development of time domain numerical simulation in large domains. This however may not be a fair conclusion to draw against the SFDTD method as it is not implemented in 3D, further study is required to confirm the efficiency difference between PSTD and SFDTD.

The figure below shows a summary of the code profiling information for an SFDTD simulation of a 5m by 4m domain with maximum frequency of 1kHz, executing for 0.2s:

SFDTD2Dfun (Calls: 2400, Time: 30.530 s)

Generated 16-May-2017 10:00:34 using performance time.
 function in file C:\Gits\IndiEngiSchola\Matlab\SFDTD\SFDTD2Dfun.m
[Copy to new window for comparing multiple runs](#)

<input checked="" type="checkbox"/> Show parent functions	<input checked="" type="checkbox"/> Show busy lines	<input checked="" type="checkbox"/> Show child functions
<input checked="" type="checkbox"/> Show Code Analyzer results	<input checked="" type="checkbox"/> Show file coverage	<input checked="" type="checkbox"/> Show function listing

Parents (calling functions)

Function Name	Function Type	Calls
SFDTD2Dtesting	script	2400

Lines where the most time was spent

Line Number	Code	Calls	Total Time	% Time	Time Plot
8	ux(i,i1) = ux(i,i1) - uCx*(p(i,...	17079859	2.657 s	8.7%	
47	p(i,i1) = p(i,i1) - pCx*(ux(i,...	17277992	2.646 s	8.7%	
48	- pCy*(uy(i+1, i1) - uy(i, i1)...	17277992	2.531 s	8.3%	
16	uy(i,i1) = uy(i,i1) - uCx*(p(i,...	17079859	2.523 s	8.3%	
46	if(idx(i, i1) > 0)	17669044	2.371 s	7.8%	
All other lines			17.803 s	58.3%	
Totals			30.530 s	100%	

PARSEfun2DC (Calls: 2400, Time: 11.293 s)

Generated 16-May-2017 09:58:46 using performance time.
 function in file C:\Gits\IndiEngiSchola\Matlab\SFDTD\PARSEfun2DC.m
[Copy to new window for comparing multiple runs](#)

<input checked="" type="checkbox"/> Show parent functions	<input checked="" type="checkbox"/> Show busy lines	<input checked="" type="checkbox"/> Show child functions
<input checked="" type="checkbox"/> Show Code Analyzer results	<input checked="" type="checkbox"/> Show file coverage	<input checked="" type="checkbox"/> Show function listing

Parents (calling functions)

Function Name	Function Type	Calls
SFDTD2Dtesting	script	2400

Lines where the most time was spent

Line Number	Code	Calls	Total Time	% Time	Time Plot
13	idx = imfilter(temp2,PSF,'symm...	2400	7.922 s	70.2%	
5	PSF = fspecial('gaussian',7,10...	2400	2.470 s	21.9%	
11	temp2(temp2 > 1) = 1;	2400	0.369 s	3.3%	
9	temp2 = floor(temp);	2400	0.276 s	2.4%	
7	temp = abs(p) ./ threshold;	2400	0.181 s	1.6%	
All other lines			0.074 s	0.7%	
Totals			11.293 s	100%	

Children (called functions)

Function Name	Function Type	Calls	Total Time	% Time	Time Plot
imfilter	function	2400	7.624 s	67.5%	
fspecial	function	2400	2.010 s	17.8%	
Self time (built-ins, overhead, etc.)			1.659 s	14.7%	
Totals			11.293 s	100%	

Figure 5.6: Code execution time profile of SFDTD functions

These results show that in the SFDTD method which includes extra steps on top of those in the FDTD method, most time is spent differentiating the matrices as opposed to filtering the domain. It is not possible in this case to compare this performance to the 3D FDTD and PSTD method as discussed above, but these results may suggest that SFDTD is worthy of further research.

Chapter 6

Conclusion and Further Work

6.1 Conclusion

The aim of this study was to evaluate three time domain numerical methods for solving the wave equation, with respect to the execution speed of each method when solving for large domains. The finite difference time domain method as presented by Hill [4] and pseudospectral time domain method presented by Angus [21] for solving the acoustic wave equation were both implemented as Matlab scripts and function. The sparse finite difference time domain method was explored, with a novel method for generating the windowing matrix that broke away from the original computational electromagnetics work by Doerr [26].

In this document the acoustic wave equation was introduced, and some equations of interest in large room acoustics were discussed. It was suggested for large room acoustic analysis in simple spaces, that modal interaction may not be of interest as few modes are likely to occur below the Schroeder frequency even in particularly reverberant environments. However, the sound level, time of arrival and direct to reverberant ratio information near the boundaries of these domains may be of considerable interest in sound system engineering applications. This may be particularly true where ray tracing models have limited accuracy and computational benefits over wave methods, due to the large number of rays required in large simulations with multiple sound source and receiver locations.

The finite difference time domain method, sparse finite difference time domain method and pseudospectral time domain methods are then described mathematically and programmatically. This includes consideration of partially absorbing boundary conditions and different sound source types. Due to constraints on this project only soft sources and simple geometries were implemented, however literature is available considering more complex geometries for both the finite difference and pseudospectral methods.

The implementations of the three methods were tested for validity. It was shown that all three methods had appropriate wave propagation behaviour. Finally the execution speed for each method with a series of increasingly larger domains was then measured recorded and analysed. It was shown that as domain size doubled in all dimensions, the time step execution time of the finite difference method increased significantly. In comparison, the time step execution speed for the pseudospectral method was a factor of 10 quicker in all but the smallest domain case tested. It was highlighted that the execution speed difference between the two methods was due not only to the difference in time and spatial step, but in the speed of executing the differentiation. As the sparse finite difference method was not successfully implemented in 3D, it was not possible to compare execution speed to the two other methods. However it could be seen that for the early portions of the execution time for each domain size, time step execution speed was reduced to below a nominal rate, and that this reduction increased as domain size increased.

6.2 Further Work

Due to the basic nature of the implementations in this study, there is naturally a significant amount of further work to do in terms of improving these implementations. Many of these improvements are not listed below, but can be found by a brief review of much of the literature referenced in this report. The list below contains brief descriptions of a small section of the further work that could be drawn from this study.

- More detailed validation of the current model implementations is required to show that the models truly represent an accurate approximation of room acoustics. The validation method presented in this report was significantly limited and requires major reconsideration.
- A deep study of 3D filtering could benefit implementation of the 3D PSTD method and the 3D SFDTD method, as both methods rely on different filtering methods across the domain during the solving process.
- As the execution speed of the SFDTD method appears quite promising for the improvement of execution speed, a 3D implementation of the SFDTD method presented in this work may be work working on. This is not a trivial undertaking due to the complexity of 3D adaptive windowing.
- Implementation of all three methods using GPGPU computing may be advantageous. However, GPGPUs are often built with single precision architecture and a double precision arbitration mechanism. So a deeper review of single and double precision implementations such as that denoted by [39] would need to also be undertaken.
- Domain decomposition such as that used in the OpenPSTD project [31] may be a great improvement for execution speed for all three methods, as this will reduce single matrix sizes and the way memory is accessed for differentiation.

- The PSTD method may only be appropriate for smooth media, and may not interact well with obstacles due to the aliasing caused by discontinuity. An implementation of PSTD for the main domain areas with FDTD handling boundaries and obstacles may provide a way to have faster time step execution and higher accuracy in the main domain body, with the simple boundary handling available in FDTD.

Bibliography

- [1] D Botteldooren. Finite-difference time-domain simulation of low-frequency room acoustic problems. *The Journal of the Acoustical Society of America*, 98(6):3302, 1995.
- [2] Jelle Van Mourik and Damian T Murphy. Hybrid Acoustic Modelling of Historic Spaces Using Blender. (c):7–12, 2014.
- [3] David Oliva Elorza. *Room acoustics modeling using the ray- tracing method : implementation and evaluation*. PhD thesis, University of Turku, 2005.
- [4] Adam J Hill. Analysis , Modeling and Wide-Area Spatiotemporal Control of Low-Frequency Sound Reproduction. (January), 2012.
- [5] J H Rindel. The use of computer modeling in room acoustics. *Journal of Vibro-engineering - Paper of the International Conference BALTIC-ACOUSTIC 2000*, 3(4):219–224, 2000.
- [6] Nicolas Tsingos. Pre-computing geometry-based reverberation effects for games Nicolas. *Aes 35Th International Conference*, 2009.
- [7] Holger Schmalle, Dirk Noy, Stefan Feistel, Gabriel Hauser, Wolfgang Ahnert, and John Storyk. Accurate Acoustic Modeling of Small Rooms. *Audio Engineering Society*, 2011.
- [8] Michael Monks, Byong Mok Oh, and Julie Dorsey. Acoustic Simulation and Visualization using a New Unified Beam Tracing and Image Source Approach. 4355, 1996.
- [9] Mads Herring Jensen. Modeling Acoustics Applications with COMSOL Multiphysics ®, 2016.
- [10] L L Beranek. *Acoustics*. McGraw-Hill electrical and electronic engineering series. McGraw-Hill, 1st edition, 1954.
- [11] T. D. Rossing. Springer Handbook of Acoustics. *Book*, (JANUARY 2007):1182, 2007.
- [12] S W Rienstra and A Hirschberg. An Introduction to Acoustics. *Physics Today*, 5(11):24, 2004.

- [13] Don Davis and Eugene Patronis. *Sound System Engineering*. Focal Press, New York, 4th edition, 2014.
- [14] F. Alton Everest and Neil A. Shaw. *Master Handbook of Acoustics, 5th Edition*, volume 110. 5th edition, 2009.
- [15] Leo L. Beranek. Analysis of Sabine and Eyring equations and their application to concert hall audience and chair absorption. *J. Acoust. Soc. Am.*, 120(3):1399–1410, 2006.
- [16] Stefan Bilbao. *Wave and Scattering Methods for Numerical Simulation*. John Wiley & Sons, 1st edition, 2004.
- [17] John B Schneider. Understanding the Finite-Difference Time-Domain Method. pages 1–403, 2015.
- [18] Kane S Yee. Numerical solution of initial boundary value problems involving Maxwell’s equations in isotropic media. *IEEE Transactions on Antennas and Propagation*, 14(3):302–307, 1966.
- [19] D Botteldooren. Acoustical finite-difference time-domain simulation in a quasi-Cartesian grid. *Acoustical Society of America*, 95(5):2313–2319, 1993.
- [20] Soren Krarup Olesen. Low Frequency Room Simulation using Finite Difference Equations. *Proceedings of the 102nd Audio Engineering Society Convention*, 1997.
- [21] Jamie A S Angus and Andrew Caunce. A GPGPU Approach to Improved Acoustic Finite Difference Time Domain Calculations. *128th Audio Engineering Society Convention*, 2010.
- [22] Tetsuya Sakuma, Shinichi Sakamoto, and Toru Otsuru. *Computational simulation in architectural and environmental acoustics: Methods and applications of wave-based computation*, volume 9784431544. 2014.
- [23] Stefan Bilbao. *Numerical Sound Synthesis: Finite Difference Schemes and Simulation in Musical Acoustics*. 2009.
- [24] Jelle Van Mourik and Damian Murphy. Explicit higher-order FDTD schemes for 3D room acoustic simulation. *IEEE/ACM Transactions on Speech and Language Processing*, 22(12):2003–2011, 2014.
- [25] Brian Hamilton and Stefan Bilbao. Fourth-Order and Optimised Finite Difference Schemes for the 2-D Wave Equation. *Research.Ed.Ac.Uk*, 2(2):1–8, 2013.
- [26] Christopher Doerr. Sparse Finite Difference Time Domain Method. *IEEE Photonics Technology Letters*, 25(23):1–1, 2013.
- [27] C Doerr. SPARSE FINITE-DIFFERENCE TIME DOMAIN SIMULATION, 2014.

- [28] J W Schuster, K C Wu, R R Ohs, and R J Luebbers. Application of moving window FDTD to predicting path loss over forest covered irregular terrain. *IEEE Antennas and Propagation Society Symposium, 2004.*, pages 1607—1610 Vol.2, 2004.
- [29] Gerard Blanchet and Maurice Charbit. *Digital Signal and Image Processing using MATLAB*. 2006.
- [30] Jukka Saarela, Jonathan Botts, Brian Hamilton, and Lauri Savioja. Audibility of dispersion error in room acoustic finite-difference time-domain simulation as a function of simulation distance. *The Journal of the Acoustical Society of America*, 139(4):1822–1832, 2016.
- [31] Maarten Hornikx, Thomas Krijnen, and Louis Van Harten. OpenPSTD: The open source pseudospectral time-domain method for acoustic propagation. *Computer Physics Communications*, 203:298–308, 2016.
- [32] Steven a. Orszag. Numerical simulation of incompressible flows within simple boundaries: accuracy. *Journal of Fluid Mechanics*, 49(01):75, 1971.
- [33] Heinz-Otto Kreiss and Joseph Oliger. Comparison of accurate methods for the integration of hyperbolic equations. *Tellus*, 24(3):199–215, 1972.
- [34] Lloyd N Trefethen. Spectral Methods in Matlab. *Lloydia Cincinnati*, 10:184, 2000.
- [35] R Rumpf. The Perfectly Matched Layer (PML) Review of Lecture 12, 2012.
- [36] Jean P Berenger. A perfectly matched layer for the absorption of electromagnetic waves. *J. Comput. Phys.*, 114:185–200, 1994.
- [37] Qing-Huo Liu and Jianping Tao. The perfectly matched layer for acoustic waves. *J. Acoust. Soc. Am.*, 102(4):2072–2082, 1997.
- [38] Carlos Spa, Jose Escolano, and Adan Garriga. Semi-empirical boundary conditions for the linearized acoustic Euler equations using Pseudo-Spectral Time-Domain methods. *Applied Acoustics*, 72(4):226–230, 2011.
- [39] Damian T Murphy, Alex Southern, and Lauri Savioja. Source excitation strategies for obtaining impulse responses in finite difference time domain room acoustics simulation. *Applied Acoustics*, 82:6–14, 2014.
- [40] Wolfgang Ahnert and Stefan Feistel. Simulation, Auralization and their Verification of Acoustic Parameters using Line Arrays. *119th Convention of the Audio Engineering Society*, 2005.
- [41] Nicolas Tsingos, Ingrid Carlbom, Gary Elko, Robert Kubli, and Thomas Funkhouser. Validating acoustical simulations in the Bell Labs Box. *IEEE Computer Graphics and Applications*, 22(4), 2002.

- [42] a. Foteinou, D. Murphy, and a. Masinton. Verification of Geometric Acoustics-Based Auralization Using Room Acoustics Measurement Techniques. *128th Audio Engineering Society Convention*, pages 1–12, 2010.
- [43] Alex Southern, Samuel Siltanen, Damian T. Murphy, and Lauri Savioja. Room impulse response synthesis and validation using a hybrid acoustic model. *IEEE Transactions on Audio, Speech and Language Processing*, 21(9):1940–1952, 2013.
- [44] Mark Thomas. Maximum Sequence Length. pages 1–9, 2007.
- [45] Peter D. Welch. The Use of Fast Fourier Transform for the Estimation of Power Spectra: A Method Based on Time Averaging Over Short, Modified Periodograms. *IEEE Transactions on Audio and Electroacoustics*, 15(2):70–73, 1967.

Appendix A

Code Listing

On request of the supervisor for this project, program code listing is not included in this document. Instead, the programs can be found on the accompanying DVD and on Github at the following address:

<https://github.com/SEDur/IndiEngiSchola>